Mon. Not. R. Astron. Soc. **393,** 1408–1422 (2009) doi:10.1111/j.1365-2966.2008.14222.x

Infrared photometric study of type II quasars

P. S. Chen★ and H. G. Shan

National Astronomical Observatories/Yunnan Observatory, Chinese Academy of Sciences, Kunming 650011, China

Accepted 2008 November 8. Received 2008 November 7; in original form 2008 July 25

ABSTRACT

For this paper, we collected almost all of the type II quasars so far discovered. Among them, 485 sources have photometric data at *JHK* bands, mainly from Two-Micron All-Sky Survey observations, 65 sources have *IRAS* photometric data in at least one of the three *IRAS* bands at 25, 60 and 100 μm and 15 sources have *IRAS* photometric data in all three *IRAS* bands. We find that in nearly half of all type II quasars, both the near- and far-infrared radiations are dominated by starlight or thermal reprocessing of starlight by dust in the underlying galaxy. The infrared radiation of the other group (slightly over half) is dominated by a non-thermal radiation in the near-infrared, and mostly in the far-infrared also (although there is a mixture particularly for the longer wavelengths). It is proposed that for the later group, hidden broad lines may exist in the infrared. On the basis of our and previous results, we also discuss the possibility that there are two distinct classes of type II quasars: 'true' type II quasars without a broad-line region and heavily obscured type I quasars, in full analogy with the case for type II Seyfert galaxies. No relationships can be found for either the near-infrared or the far-infrared colours and the redshift. Correlations between absolute magnitude in the near- and far-infrared with redshift are found, but could be due to a flux limit (Malmquist bias).

Key words: galaxies: photometry – quasars: general – infrared: galaxies.

1 INTRODUCTION

The unified scheme for active galactic nuclei is widely accepted. Briefly, the physics of black hole, accretion disc, jet and obscuring torus is convolved with the geometry of the viewing angle and can explain most of the apparent disparate properties of active galaxies (Antonucci 1993; Urry & Padovani 1995; Norman et al. 2002). However, its general application in its simplest form has been strongly questioned from very diverse observational evidence (e.g. Dultzin-Hacyan et al. 1999; Tran 2001; Krongold & Dultzin-Hacyan 2002; Krongold, Dultzin-Hacyan & Marziani 2003; Koulouridis et al. 2006b; Dultzin et al. 2008; Storchi-Bergmann 2008). Observationally, for active galactic nuclei, type I objects exhibit the straight physics of active galactic nuclei without absorption, and type II objects arise when the view is obscured by the torus (Norman et al. 2002). Many type I Seyfert galaxies with unobscured broad lines and type II Seyfert galaxies with narrow high-ionization lines have been found over many years. Besides type I quasars (typically Paloma–Green, hereafter PG, quasars), so called type II quasars, heavily obscured by the torus with a large viewing angle, were sought.

According to the unified scheme, a type II quasar would consist of a quasar with the axis of symmetry almost perpendicular to our line of sight, so that the torus around the accretion disc would be viewed edge-on, obscuring the central region of the source. Therefore, type II quasars should have a significant fraction of their bolometric luminosity in the infrared. In addition, a part of the ultraviolet and optical continuum in the core region would be thermally reprocessed by circumnuclear dust in the torus. Thus, investigation of radiation in the infrared is very important for type II quasars.

The first type II quasar, IRAS 09104+4109, was discovered by Kleinmann et al. (1988). However, before 2002, only about a dozen type II quasars had been found because they are very faint in the optical. In longer wavelengths, type II quasars are rather easily found because of their strong radiation at such wavelengths. After 2002, several tens of type II quasars were been found by infrared, radio and submillimetre selection criteria (e.g. Schmidt et al. 2002; Gregg et al. 2002; Lacy et al. 2004; Dadina & Cappi 2004; Mainieri et al. 2005; Lacy et al. 2005; Martinez-Sansigre et al. 2006; Leipski et al. 2007). For example, Lacy et al. (2004, 2005) used the criterion of $\log(L_{5\,\mu m}/\mathrm{W\,Hz^{-1}}) \geq 23.6$ to identify type II quasars.

In addition, type II quasars are expected to have hard X-ray spectra because the gas along the line of sight absorbs soft X-rays and permits only hard X-rays from the nucleus to escape directly (Zakamska et al. 2003). In fact, since 2002 many type II quasars with $L_{2-8\,\mathrm{KeV}} > 10^{44}$ erg s^{-1} and absorbing column $>10^{22}$ cm^{-2} in hard X-ray spectra have been found (e.g. Gilli et al. 2002; Norman et al. 2002; Stern et al. 2002; Barger et al. 2003; Della Ceca et al. 2003; Gandhi et al. 2004; Szokoly et al. 2004; Caccianiga et al. 2004; Mainieri et al. 2005; Maiolino et al. 2006; Punsly 2006; Vignali, Alexander & Comastri 2006; Gandhi, Fabian & Crawford 2006;

★E-mail: iraspsc@yahoo.com.cn

Sturm et al. 2006). To date, the number of X-ray selected type II quasars is nearly 100.

The Sloan Digital Sky Survey (SDSS; York et al. 2000; Stoughton et al. 2002) is a large imaging and spectroscopic survey which, when completed, will cover about a quarter of the extragalactic sky with photometric magnitude limits down to about 21–22 in the 3550–8900 Å region and spectroscopic magnitude limits of S/N = 4.5 pixel^{-1} at $\lambda f_\lambda = 10^{-13}$ erg cm^{-2} s^{-1} in the 3800–9200 Å region. As it is so large and sensitive, about 10^6 galaxies and quasars are included in the survey. The SDSS therefore makes it possible to find a large number of type II quasar candidates. In fact, Zakamska et al. (2003, 2004, 2005, 2006) and Ptak et al. (2006), mainly using the high-ionization line selection criteria, found 132 type II quasars with $\log(L_{[\mathrm{O\,III}]\,\lambda5007}/\mathrm{L}_\odot) > 8.48$ (equivalent to $M_\mathrm{B} < -23$). Very recently, Reyes et al. (2008) presented a catalogue of type II quasars with $\log(L_{[\mathrm{O\,III}]\,\lambda5007}/\mathrm{L}_\odot) > 8.3$ from SDSS based on optical emission lines. The catalogue contains 887 type II quasars with redshifts $z < 0.83$ including almost all sources found by Zakamska et al. (2003, 2004, 2005, 2006) and Ptak et al. (2006). Thus, the number of type II quasars found to date is about 1000.

In summary, type II quasars should be objects with: (i) type II Seyfert galaxies – like spectra and (ii) luminosities either in the optical as $\log(L_{[\mathrm{O\,III}]\,\lambda5007}/\mathrm{L}_\odot) > 8.3$ or in the infrared as $\log(L_{5\,\mu\mathrm{m}}/\mathrm{WHz}^{-1}) \geq 23.6$, as well as in the X-ray band as $L_{2-8\,\mathrm{KeV}} > 10^{44}$ erg s^{-1}.

In this paper, we collected about 1000 type II quasars from the literature. Among them, 485 sources have photometric data at *JHK* bands, 65 sources have *IRAS* photometric data at least in one of the three *IRAS* bands at 25, 60 and 100 μm, and 15 sources have *IRAS* photometric data in all three *IRAS* bands. Infrared properties for the above sample are discussed mainly using Two-Micron All-Sky Survey (2MASS) and *IRAS* photometric data.

2 WORKING SAMPLE AND DATA PROCSSING

2.1 Working sample

We collected about 1000 type II quasars from the literature as mentioned in Section 1. Among them, 485 sources listed in Table 1 have photometric data at *JHK* bands. In addition, 65 sources listed in Table 2 have *IRAS* photometric data in at least one of three *IRAS* bands. Those sources are our working sample.

2.2 Near-infrared counterpart identifications

First of all, coordinates from the original papers were used to make cross-identifications of 2MASS counterparts. In practice, the maximum positional uncertainty in 2MASS was considered as the upper limit to restrict the cross-identifications. If there is more than one source within the searching area, the closest one with appropriate colour is selected as the counterpart. 473 sources were found to have 2MASS data. Furthermore, 12 sources from Soifer et al. (1991), Norman et al. (2002), Beichman et al. (2003) and Gandhi et al. (2004) have additional data at *JHK* bands. All sources having near-infrared data are listed in Table 1. In Table 1, the items listed are: (i) the source number from Reyes et al. (2008); (ii) the name of source if other than from Reyes et al. (2008); (iii) the redshift; (iv) and (v) coordinates in the epoch of 2000 from 2MASS or the original reference with symbol '#'; (vi)–(xi) magnitudes and magnitude uncertainties at *JHK* bands; (xii) the derived $E(B-V)$ and (xiii) the note: the original references if other than from Reyes et al. (2008) are shown.

2.3 Galactic interstellar extinction correction

Corrections for the interstellar extinction caused by our Galaxy, $E(B-V)$, can be obtained from the maps given by Schlegel, Finkbeiner & Davis (1998). In fact, $E(B-V)$ can be directly obtained through the NASA/IPAC Extragalactic Database (NED Home Page) for all sources. Then from Schlegel et al. (1998), $A_J = 0.272\,A_v$, $A_H = 0.173\,A_v$ and $A_K = 0.110\,A_v$ can be derived. Actually in the regions with $|b| \geq 30°$, the $E(B-V)$ is usually quite small, and as shown above, the interstellar extinction coefficients at *JHK* bands are just equal to about 1/4 to 1/10 of A_v. In addition, if the uncertainties of the measured magnitudes from 2MASS or other resources given in Table 1 are taken into account, then most sources with $|b| \geq 30°$ have interstellar extinction coefficients at *JHK* bands smaller than the uncertainties of the measured magnitudes. More than 90 per cent of the sources are located at $|b| \geq 30°$, therefore interstellar extinction corrections are made for just a small number of sources. In the following discussions, the magnitudes used at *JHK* bands are all corrected for Galactic interstellar extinction according to the methods mentioned here.

3 NEAR-INFRARED PROPERTIES

3.1 Near-infrared two-colour diagram

After Galactic interstellar extinction corrections for magnitudes at *JHK* bands in Table 1, the $(J-H)-(H-K)$ diagram for 433 type II quasars with the proper magnitude uncertainty at all *JHK* bands is plotted in Fig. 1. In addition, about 60 typical type II Seyfert galaxies and 40 type I quasars (PG quasars) with the similar redshifts to the type II quasars are selected from Polletta et al. (1996) and Schmidt & Green (1983), respectively. According to the procedure mentioned in Section 2, all 2MASS counterparts of those type II Seyfert galaxies and PG quasars are also identified and the Galactic interstellar extinction corrections are also made for them. The reason for selecting samples of type II Seyfert galaxies and PG quasars here is that those sources have similar redshift range to the type II quasars in this paper. In addition, the power law ($F = \nu^{-\alpha}$) and the blackbody distributions, respectively, are also shown in Fig. 1. The power-law line in Fig. 1 is derived in such a way that in a certain wavelength range $\Delta\lambda = \lambda_2 - \lambda_1 (\lambda_1 < \lambda_2)\,\alpha$ is the spectral index, then

$$m(\lambda_1) - m(\lambda_2) = -2.5 \log\left[(\lambda_1/\lambda_2)^\alpha (S_{\lambda2}/S_{\lambda1})\right], \quad (1)$$

where $m(\lambda_1)$ and $m(\lambda_2)$ are magnitudes at wavelengths λ_1 and λ_2, respectively. $S_{\lambda1}$ and $S_{\lambda2}$ are absolute flux calibrations at wavelengths λ_1 and λ_2, respectively. According to Cohen et al. (2003), for the 2MASS photometric system, $S_J = 1594$ Jy, $S_H = 1024$ Jy and $S_K = 666.7$ Jy. Therefore for some given values of α, the colours $m(\lambda_1) - m(\lambda_2)$ can be obtained. According to formula (1), taking $m(\lambda_1) - m(\lambda_2)$ as $J-H$ and $H-K$, respectively, the power-law line can be determined and this is shown in Fig. 1. The blackbody line in Fig. 1 is derived according to the calculation of the Plank function in two wavelengths (frequencies) and a certain temperature around this wavelength interval, i.e.

$$m(\lambda_1) - m(\lambda_2) = -2.5 \log[(B_{\lambda1}/B_{\lambda2})(S_{\lambda2}/S_{\lambda1})], \quad (2)$$

where $B_{\lambda1}$ and $B_{\lambda2}$ are the Plank functions with same temperature T at λ_1 and λ_2, respectively. According to formula (2), taking

Table 1. Near-infrared observation of type II quasars.

No. Name	Z	RA (2000, 2MASS)	Dec.	J	J_e	H	H_e	K	K_e	E(B − V)	Note
2	0.2689	000351.80	−010142.1	16.752	0.151	15.930	0.154	15.123	0.150	0.03	∗
6	0.0999	001126.95	+155329.9	15.973	0.084	15.180	0.088	14.956	0.147	0.06	
7	0.1668	001206.30	−094725.4	16.454	0.135	15.699	0.133	14.990	0.128	0.03	∗
8	0.3600	002016.90	−093245.0	17.005	0.162	16.374	0.232	15.626	0.212	0.04	∗
11	0.1888	002727.85	−084918.3	16.055	0.111	15.021	0.139	14.525	0.109	0.03	
12	0.2028	002751.90	+144721.9	16.305	0.115	15.289	0.115	14.568	0.084	0.05	
14	0.3103	002852.86	−001435.6	15.975	0.117	15.258	0.121	14.615	0.128	0.02	
15	0.2626	003304.78	−002425.1	16.551	0.110	15.768	0.118	15.341	0.180	0.01	
17	0.1738	003356.45	−004521.6	16.308	0.100	15.584	0.099	14.802	0.105	0.02	∗
19	0.0950	004113.76	−095231.6	15.256	0.089	14.580	0.103	14.175	0.094	0.03	
20	0.1175	004252.57	+153246.8	14.824	0.067	14.170	0.071	13.601	0.062	0.06	
23	0.1329	004741.47	+004129.3	16.107	0.122	15.252	0.124	14.707	0.110	0.02	
26	0.1348	005230.62	−011548.4	16.399	0.130	15.670	0.139	15.113	0.162	0.05	
29	0.1880	010205.72	+144325.8	15.590	0.073	14.977	0.112	14.270	0.085	0.09	∗
30	0.2021	010315.91	+002918.2	16.071	/	15.923	0.220	14.551	/	0.03	
31	0.3144	010348.58	+003932.2	17.098	0.194	16.027	0.175	15.224	0.159	0.03	
37	0.3891	011429.55	+000036.4	17.255	0.240	16.042	0.205	15.200	0.140	0.02	
/ SDSS J0115+0015	0.390	011522.18	+001518.8	17.077	0.198	15.746	0.169	15.062	0.151	0.02	(2)
39	0.1251	011935.62	−102613.0	15.968	0.087	15.259	0.117	14.660	0.118	0.03	
40	0.6331	011950.73	+000736.3	17.180	0.212	16.436	0.251	15.622	0.215	0.03	∗
43	0.1969	012234.24	−104605.3	15.931	0.099	15.256	0.107	14.404	0.093	0.04	∗
867	0.7111	012925.82	−005900.1	16.827	0.159	15.765	/	14.870	/	0.02	
47	0.1969	013942.13	−000618.8	16.590	0.123	16.068	0.211	15.257	0.169	0.02	∗
48	0.1442	014124.91	−094518.9	13.953	0.039	13.400	0.044	13.145	0.049	0.02	
/ FIRST 0134−0931	2.216	013435.67	−093103.0	16.187	0.131	14.793	0.074	13.579	0.055	0.02	∗ (17)(18)
52	0.1973	014700.06	+135213.7	16.712	0.140	16.015	0.150	15.631	0.202	0.05	
54	0.4204	015130.07	+000326.4	14.800	0.036	14.256	0.042	13.947	0.051	0.03	
55	0.2413	015341.03	−010945.1	16.819	0.164	15.676	0.140	15.264	0.166	0.02	
56	0.1628	015344.33	−085715.2	16.080	0.094	15.177	0.106	14.361	0.093	0.02	∗
62	0.0859	020223.72	+124717.8	15.356	0.083	14.501	0.081	13.673	0.071	0.08	∗
66	0.2324	021716.29	−085652.6	16.549	0.147	15.723	0.157	15.276	0.181	0.02	
74	0.1001	023224.26	−081140.3	15.288	0.059	14.565	0.053	14.129	0.076	0.03	
/ SDSS J0233+0040	0.388	023359.93	+004012.7	17.017	0.158	16.825	/	15.624	0.176	0.03	(3)
76	0.2066	023635.07	+005126.8	16.176	0.098	15.169	0.095	13.940	0.059	0.03	∗
80	0.2027	024612.97	+000439.1	16.581	/	15.829	/	15.186	0.169	0.03	
83	0.4080	024946.09	+001003.9	17.094	0.218	16.189	0.195	15.536	0.180	0.05	
89	0.2508	030439.85	−005203.4	17.073	0.215	16.439	0.244	15.464	0.171	0.08	∗
91	0.3666	030647.55	−004414.6	17.343	0.229	16.174	0.197	15.428	0.212	0.09	
93	0.2075	031428.26	−072517.8	16.389	0.106	15.421	0.097	14.557	0.090	0.08	∗
95	0.2742	031547.08	−075938.7	16.774	0.152	15.890	0.158	14.989	0.139	0.08	∗
98	0.1572	031722.23	+004801.0	15.729	0.100	14.936	0.107	14.133	0.094	0.08	∗
99	0.1173	031752.90	−005417.5	15.729	0.098	15.137	0.124	14.336	0.108	0.10	∗
105	0.2381	032712.53	−011510.2	16.104	0.110	15.560	0.150	14.743	0.126	0.10	∗
106	0.2083	033100.47	−000419.5	16.609	0.151	16.047	0.175	15.425	0.183	0.10	∗
/ CDFS 202	3.700	033229.86	−275105.8#	23.28	0.15	/	/	20.97	0.11	0.01	(4),*JHK*(4)
107	0.3098	033248.51	−001012.7	16.581	0.109	15.784	0.114	14.698	0.112	0.08	∗
873	0.4317	033606.68	−000754.7	17.249	0.198	16.431	0.204	15.737	0.238	0.08	∗
110	0.0848	033923.15	−054841.5	15.968	0.079	15.402	0.107	14.840	0.111	0.05	∗
/ AX J0341.4-4453	0.672	034124.46	−445300.9	16.728	0.152	15.851	0.135	14.518	0.088	0.01	∗ (19)
118	0.3081	034602.56	−000058.8	16.576	0.127	15.915	0.157	15.087	0.158	0.18	∗
120	0.1649	035024.55	+005852.7	15.584	0.100	14.908	0.103	14.082	0.109	0.18	∗
122	0.1705	040001.59	−065254.1	15.578	0.072	14.871	0.107	13.916	0.069	0.08	∗
123	0.3204	040152.34	−053228.7	17.186	0.186	16.426	0.203	15.768	0.248	0.09	∗
124	0.3476	040456.43	−042323.4	16.452	/	16.175	0.212	14.977	0.131	0.10	
/ 2MASS 044114	0.236	044114.05	−373436.9	16.629	0.130	15.521	0.127	14.797	0.117	0.01	(20)
126	0.1103	073142.39	+392623.8	15.787	0.076	15.153	0.078	14.311	0.060	0.05	∗
/ 3C 183	2.429	073522.45	+434424.8	16.200	0.087	15.613	0.119	15.231	0.114	0.05	(5)
127	0.3563	073555.68	+422035.1	18.030	/	17.136	/	15.299	0.116	0.05	
/ FIRST 0738+2750	1.985	073820.12	+275045.6	17.045	0.143	16.210	0.133	15.276	0.123	0.04	∗ (17)
130	0.2972	073849.75	+315611.5	17.050	0.203	16.056	0.196	15.088	0.130	0.04	∗
132	0.1499	074054.00	+342234.4	16.446	0.115	15.570	0.110	15.266	0.135	0.04	
133	0.2102	074129.67	+392835.9	16.114	0.100	15.213	0.093	14.540	0.092	0.05	
136	0.1973	074433.10	+201102.6	16.166	0.082	15.505	0.107	14.882	0.090	0.05	∗
138	0.1807	074714.63	+424520.2	16.101	0.099	15.626	0.120	15.026	0.115	0.05	∗

Table 1 – *continued*

No. Name	Z	RA (2000, 2MASS)	Dec.	J	J_e	H	H_e	K	K_e	E(B − V)	Note
140	0.2800	074751.59	+320051.4	16.873	0.148	16.029	0.170	15.213	0.123	0.06	*
141	0.1315	074948.34	+264734.3	16.040	0.093	15.418	0.117	14.817	0.116	0.03	*
142	0.2390	075226.52	+251020.2	16.425	0.144	15.291	0.123	14.744	0.116	0.11	
143	0.0969	075324.39	+384731.7	15.463	0.074	14.675	0.076	14.258	0.080	0.04	
146	0.1789	075605.21	+381651.3	15.953	0.094	15.593	0.164	14.501	0.101	0.04	*
148	0.2160	075820.97	+392335.8	16.801	0.134	16.058	0.146	15.223	0.124	0.05	*
151	0.0544	075940.97	+505024.1	14.500	0.049	13.857	0.062	13.295	0.042	0.04	
153	0.3999	080019.10	+183556.8	16.777	0.149	15.763	/	15.704	0.187	0.03	
155	0.0766	080218.65	+304622.9	14.923	0.051	14.071	0.055	13.580	0.050	0.04	
156	0.1206	080224.34	+464300.8	15.183	0.060	14.633	0.076	13.833	0.059	0.07	*
157	0.2384	080234.12	+372801.2	16.162	0.103	15.324	0.127	14.733	0.097	0.04	
158	0.0811	080252.93	+255255.7	14.168	0.058	13.491	0.073	12.949	0.057	0.03	
159	0.0656	080337.33	+392633.1	14.140	0.045	13.447	0.051	13.135	0.051	0.04	
161	0.3010	080353.78	+171133.8	16.617	0.163	15.907	0.213	15.410	0.196	0.02	
164	0.1284	080523.31	+281815.5	15.121	0.088	14.538	0.141	13.925	0.092	0.04	*
166	0.1526	081034.87	+385610.1	15.832	0.076	15.285	0.102	14.699	0.098	0.04	*
167	0.1829	081100.22	+444216.5	15.575	0.066	14.947	0.079	14.436	0.077	0.04	
168	0.2333	081118.09	+244935.3	16.027	0.075	15.322	0.083	14.838	0.096	0.04	
171	0.2529	081246.28	+384526.7	16.263	0.123	15.709	/	15.039	0.133	0.03	
174	0.2707	081354.20	+161118.2	16.304	0.123	15.559	0.146	15.139	0.152	0.03	
177	0.1244	081420.81	+303050.5	15.705	0.076	15.123	0.088	14.607	0.093	0.03	*
180	0.0758	081842.37	+360409.7	15.354	0.052	14.715	0.074	14.189	0.066	0.05	
181	0.2316	081932.98	+423610.6	16.640	0.140	15.592	0.127	14.983	0.108	0.06	
187	0.1734	082711.21	+223324.2	15.809	0.068	14.998	0.076	14.414	0.063	0.04	
188	0.3814	082751.56	+263726.7	16.974	0.183	15.991	0.171	15.501	0.171	0.06	
189	0.2274	082845.80	+414540.2	15.840	0.077	15.207	0.090	14.397	0.072	0.03	*
190	0.3443	083028.14	+202015.7	16.843	0.181	15.985	0.179	15.502	0.178	0.03	
191	0.1546	083045.21	+370946.7	15.348	0.058	14.701	0.062	13.980	0.058	0.03	*
192	0.2326	083130.32	+070559.7	16.450	0.140	15.415	0.155	14.988	0.170	0.03	
194	0.2076	083201.14	+392126.1	15.662	0.068	15.111	0.084	14.361	0.073	0.04	*
195	0.2007	083433.46	+222117.2	16.668	0.131	15.611	0.110	15.394	0.138	0.03	
196	0.2414	083454.88	+553420.7	16.366	0.157	15.263	/	14.180	/	0.04	
197	0.1660	083501.34	+313809.5	16.553	0.136	15.672	/	15.306	0.162	0.05	
199	0.3000	083512.43	+175441.3	16.494	0.147	15.885	0.148	14.869	0.112	0.03	*
200	0.1170	083523.84	+524055.0	14.690	0.052	14.060	0.068	13.476	0.059	0.03	*
201	0.1922	083528.03	+274729.3	16.213	0.097	15.694	0.140	15.106	0.125	0.03	*
202	0.1736	083647.11	+402527.4	15.797	0.086	15.285	0.118	14.388	0.071	0.04	*
204	0.2520	083716.02	+324305.3	16.476	0.132	15.474	0.110	14.961	0.129	0.04	
205	0.2068	083752.75	+445025.9	15.718	0.077	14.857	0.077	13.994	0.059	0.02	*
207	0.1437	083835.83	+441356.7	15.826	0.067	15.114	0.096	14.420	0.081	0.02	*
208	0.2635	083839.38	+444654.7	16.079	0.087	15.410	0.082	14.604	0.084	0.02	*
209	0.4298	083851.14	+252713.9	17.146	0.195	16.367	0.218	15.446	0.161	0.04	*
210	0.3375	083925.21	+343031.0	16.832	0.171	16.161	0.210	15.095	0.137	0.03	*
211	0.4246	083945.99	+384319.2	17.229	0.234	15.923	0.191	15.164	0.132	0.03	
212	0.4026	084015.48	+504342.4	16.939	0.199	15.843	0.150	15.439	0.173	0.02	
213	0.1674	084028.62	+332052.2	15.998	0.129	15.344	0.148	14.631	0.111	0.03	*
214	0.3132	084041.05	+383820.1	16.751	0.176	15.748	0.144	14.990	0.115	0.03	
219	0.1106	084135.09	+010156.0	15.879	0.116	14.913	0.122	14.499	0.159	0.04	
220	0.2748	084227.46	+054716.1	16.650	0.162	15.963	0.185	15.012	0.176	0.08	*
222 AX J0843+2942	0.3980	084309.86	+294404.9	17.069	0.178	16.399	/	15.297	0.136	0.05	
225	0.0539	084344.99	+354942.3	14.171	0.052	13.423	0.053	13.049	0.050	0.03	
230	0.1793	084749.76	+400416.1	16.390	0.115	15.606	/	14.861	/	0.02	
232	0.1843	084907.90	+362253.3	16.389	0.129	16.050	0.161	15.022	0.110	0.03	*
235	0.2395	085025.44	+412222.1	16.237	0.092	15.843	0.157	15.083	0.125	0.02	*
236	0.1787	085038.16	+303932.0	16.538	0.119	15.865	0.135	15.105	0.108	0.03	*
239	0.1882	085205.47	+024310.6	16.620	0.158	15.682	0.164	15.179	0.182	0.03	
243	0.1276	085319.48	+385239.0	14.731	0.048	13.794	0.046	12.840	0.037	0.02	*
245	0.2604	085356.81	+362455.9	16.289	0.102	15.300	0.107	14.939	0.108	0.03	
247	0.2567	085435.32	+244136.3	16.727	0.164	16.001	0.212	15.391	0.172	0.03	
248	0.1733	085441.88	+400053.5	16.214	0.104	15.767	0.146	15.051	0.110	0.02	*
249	0.2006	085510.73	+502146.2	16.345	0.125	15.662	0.149	14.644	0.087	0.02	*
251	0.3567	085554.47	+370900.7	16.793	/	15.842	/	15.211	0.144	0.03	
252	0.1387	085810.64	+312136.2	16.268	0.099	15.305	0.095	14.446	0.074	0.02	*
253	0.4538	085829.57	+441734.6	17.292	0.257	16.172	0.230	15.152	0.129	0.02	*

Table 1 – *continued*

No. Name	*Z*	RA (2000, 2MASS)	Dec.	*J*	*J*_e	*H*	*H*_e	*K*	*K*_e	*E*(*B* − *V*)	Note
255	0.2357	090036.85	+205340.5	16.636	0.144	15.883	0.143	15.179	0.134	0.02	*
256	0.4526	090157.34	+215834.9	17.256	0.199	16.446	0.215	15.872	0.227	0.02	
261	0.3291	090307.84	+021152.1	16.751	0.167	16.059	0.160	14.850	0.136	0.04	*
264	0.1511	090403.75	+074819.4	16.278	0.147	15.480	0.157	14.838	0.138	0.05	
270	0.1668	090722.32	+462018.1	15.629	0.086	14.990	0.096	14.283	0.097	0.01	*
271	0.0848	090754.08	+521127.6	15.045	0.064	14.296	0.072	13.953	0.068	0.01	
274	0.6703	090933.54	+425346.5	16.257	0.148	15.333	0.136	14.632	0.114	0.01	
275	0.1654	090935.52	+105211.0	16.601	0.161	15.740	0.171	15.213	0.185	0.04	
277	0.6032	091157.54	+014327.5	16.456	/	16.231	0.201	14.868	0.134	0.03	
280	0.2490	091307.96	+192418.7	17.142	0.177	16.269	0.160	16.120	0.233	0.04	
281 IRAS 09104+4109	0.4409	091345.46	+405628.3	16.826	0.169	15.871	0.146	14.774	0.112	0.01	*
/ IRAS 09_3	1.43	091357.5	+405939#	18.63	0.05	17.88	0.05	17.04	0.05	0.01	* (6),*JHK*(6)
283	0.1298	091544.18	+300922.1	15.206	0.052	14.388	0.052	14.088	0.059	0.02	
284	0.1422	091646.05	+283527.1	15.207	0.075	14.422	0.061	13.420	0.051	0.02	*
285	0.1564	091800.27	+042506.4	15.462	0.083	14.779	0.088	13.778	0.062	0.04	*
286	0.2400	091803.31	+285815.9	16.366	/	15.410	/	15.034	0.146	0.02	
296	0.2727	092438.25	+302837.0	16.613	0.145	15.947	0.157	14.879	0.108	0.02	*
298	0.1921	092549.17	+491651.5	16.477	0.140	15.659	0.144	15.072	0.141	0.01	
300	0.1897	092635.12	+072446.6	15.726	0.073	15.088	0.088	14.284	0.091	0.05	*
302	0.1948	092722.34	+201804.0	16.676	0.134	15.898	0.136	15.464	0.159	0.03	
303	0.1174	092907.77	+002636.8	16.008	0.111	15.031	0.101	14.056	0.072	0.03	*
304	0.1778	093204.25	+202226.9	15.991	0.090	15.109	0.091	14.677	0.083	0.04	
305	0.1453	093239.71	+410609.9	16.253	0.128	15.732	0.153	14.793	0.108	0.01	*
308	0.0956	093625.39	+592452.7	15.569	0.081	14.967	0.095	14.619	0.080	0.01	
314	0.1366	093952.78	+355358.9	15.786	0.084	15.082	0.089	14.358	0.077	0.01	*
320	0.1559	094506.41	+035551.0	16.643	0.196	15.904	0.197	15.313	0.198	0.04	
321	0.1280	094521.33	+173753.2	15.721	0.068	15.265	0.141	14.459	0.075	0.02	*
323	0.1664	094612.67	+042827.1	16.015	0.120	15.512	0.167	14.965	0.148	0.04	*
327	0.1791	094825.24	+250658.1	15.489	0.056	14.701	0.060	14.039	0.052	0.02	
334	0.1640	095851.32	+483228.9	16.297	0.102	15.571	0.106	14.819	0.104	0.01	*
335	0.1512	095856.30	+601741.5	16.233	0.150	15.558	0.153	14.901	0.112	0.01	*
337	0.1481	100013.15	+124226.2	15.737	0.082	15.145	0.102	14.172	0.070	0.03	*
338	0.1869	100154.93	+302418.4	16.334	0.102	15.895	0.143	14.799	0.101	0.01	*
339	0.2085	100202.11	+055145.3	15.949	0.101	15.395	0.119	14.801	0.132	0.02	*
344	0.1460	100327.90	+554153.5	16.294	0.099	15.715	0.118	15.229	0.132	0.01	
346	0.1204	100602.49	+071132.3	15.246	0.106	14.240	0.097	13.156	0.074	0.02	*
349	0.2229	100900.10	+132254.8	16.047	0.113	15.346	0.145	14.820	0.134	0.04	
350	0.1436	100921.26	+013334.6	15.891	0.091	15.410	0.127	14.862	0.126	0.03	*
351	0.0977	101043.35	+061201.4	14.934	0.076	13.769	0.075	12.519	0.037	0.02	*
352	0.3640	101107.96	+194910.2	17.131	0.214	15.957	0.171	15.317	0.160	0.03	
356	0.1202	101536.21	+005459.6	15.879	0.095	14.982	0.094	14.536	0.118	0.03	
357	0.1823	101623.78	+535806.1	16.268	0.114	15.284	0.106	14.898	0.099	0.01	
358	0.1765	101643.98	+073850.1	16.494	0.174	15.650	0.175	15.157	0.192	0.03	
359	0.1163	101653.83	+002857.1	15.657	0.095	15.031	0.104	14.079	0.087	0.03	*
361	0.1817	101754.73	−002811.6	16.090	0.107	15.515	0.120	14.867	0.130	0.03	*
/ A963_20	2.40	101802.4	+390007#	/	/	19.47	0.11	19.14	0.11	0.01	(6),*JHK*(6)
362	0.1563	102002.47	+072700.7	16.139	0.129	15.446	0.166	14.988	0.154	0.02	
363	0.1083	102103.79	+071056.3	15.430	0.077	14.629	0.081	14.056	0.077	0.02	
364	0.4063	102229.34	+192938.5	16.917	0.175	16.140	/	15.229	0.153	0.02	
365	0.1440	102256.99	+473454.3	15.743	0.089	15.277	0.121	14.719	0.110	0.01	*
366	0.1128	102310.97	−002810.5	16.724	0.176	16.116	0.211	14.735	/	0.04	
/ IRAS F10214+4724	2.286	102434.50	+470911#	18.65	0.15	17.15	0.10	16.37	0.10	0.01	(12)(15),*JHK*(16)
368	0.2570	102736.48	+285917.6	17.066	/	16.505	0.180	15.386	0.128	0.02	
372	0.2096	102955.10	+392047.2	16.424	0.144	15.344	0.116	14.882	0.116	0.01	
373	0.1413	102955.35	+505959.8	16.346	0.128	15.488	0.147	15.182	0.155	0.01	
374	0.1191	103252.60	+492612.7	15.776	0.084	15.055	0.086	14.660	0.098	0.01	
375	0.1277	103311.63	+013754.5	16.068	0.132	13.672	/	14.952	0.145	0.03	
377	0.0511	103408.54	+600152.1	14.094	0.095	13.280	0.087	12.652	0.045	0.01	
378	0.1507	103456.38	+393940.8	15.768	0.070	15.048	0.094	14.536	0.082	0.01	
379	0.4830	103509.28	+473721.4	17.394	0.246	16.204	0.246	15.681	0.192	0.01	
380	0.1068	103600.39	+013653.7	14.876	0.078	14.218	0.098	13.547	0.077	0.03	*
879	0.4316	103622.22	+635553.3	17.444	0.241	15.889	/	15.265	0.167	0.01	
382	0.2061	103734.21	+140120.8	15.392	0.073	14.776	0.100	13.862	0.079	0.03	*
385	0.2266	103932.85	−003419.1	16.223	0.096	15.468	0.083	14.646	0.101	0.06	*

Table 1 – *continued*

No. Name	Z	RA (2000, 2MASS)	Dec.	J	J_e	H	H_e	K	K_e	$E(B-V)$	Note
391	0.1555	104256.62	+043311.8	15.865	0.109	15.183	0.125	14.584	0.111	0.03	
393	0.2104	104426.72	+063754.0	16.333	0.125	15.974	0.213	15.026	0.155	0.03	*
/ SDSS J1045+5611	0.428	104505.35	+561118.0	17.248	0.093	16.164	0.106	15.438	0.082	0.01	(1)(3),*JHK*(7)
397	0.1447	104632.22	+543559.7	15.977	0.081	15.117	0.093	14.116	0.059	0.01	*
402	0.2235	105122.32	+463411.2	16.368	0.125	15.899	0.194	14.845	0.132	0.01	*
403	0.0522	105208.20	+060915.2	14.693	0.089	14.039	0.110	13.617	0.074	0.03	
/ LH 901A	0.205	105252.75	+572859.6	16.137	0.111	15.365	0.118	14.844	0.107	0.02	(8)
404	0.1498	105337.22	+464649.9	16.361	0.141	15.203	/	15.097	0.163	0.02	
406	0.1453	105555.34	+110252.1	15.715	0.091	15.023	0.109	14.496	0.110	0.01	
408	0.2055	105855.61	+102820.2	16.180	0.114	15.442	0.146	14.746	0.142	0.03	*
409	0.1354	105900.15	+500255.5	15.682	0.088	14.972	0.113	14.280	0.087	0.01	*
410	0.1188	105903.48	+572155.0	15.978	0.090	15.491	0.155	15.013	0.110	0.01	*
411	0.2203	105916.68	+545344.2	16.259	0.101	15.486	0.132	14.924	0.115	0.01	
412	0.1004	110012.39	+084616.2	14.895	0.083	13.970	0.104	12.850	0.051	0.03	*
413	0.1345	110033.51	+495120.1	15.706	0.090	15.082	0.102	14.431	0.085	0.01	*
416	0.0776	110212.99	+645925.1	14.478	0.043	13.652	0.047	13.004	0.040	0.03	
417	0.2855	110252.69	+531316.6	16.476	0.119	15.263	0.105	14.822	0.106	0.01	
418	0.2544	110258.85	+034652.4	16.583	0.164	15.129	/	15.339	0.206	0.05	
420	0.2097	110420.64	+483239.6	15.938	0.082	14.967	0.088	14.581	0.088	0.01	
422	0.2424	110621.99	+035747.5	16.242	0.128	15.635	0.137	15.148	0.184	0.05	
423	0.1511	110649.58	+254146.7	16.189	0.108	15.473	0.123	14.651	0.101	0.01	*
424	0.1950	110655.33	+013548.3	16.341	0.132	15.639	0.174	14.747	0.140	0.04	*
427	0.2177	110835.93	+072559.9	16.566	0.156	15.838	0.188	15.330	0.200	0.03	
428	0.1815	110851.03	+065901.3	15.634	0.090	15.025	0.080	14.289	0.087	0.03	*
430	0.3275	110938.06	+265959.3	17.245	0.204	16.393	0.183	15.588	0.176	0.02	*
431	0.2612	110952.83	+423315.9	16.543	0.125	15.835	0.133	15.064	0.114	0.01	*
432	0.1095	111006.28	−010116.3	16.466	0.105	15.964	0.135	15.392	0.181	0.03	*
434	0.0904	111100.60	−005335.0	14.696	0.076	13.826	0.085	13.207	0.062	0.03	
436	0.1628	111148.31	+111542.8	15.798	0.086	15.140	0.116	14.595	0.117	0.02	
437	0.3966	111238.41	+121024.6	17.147	0.199	16.501	0.264	15.420	0.168	0.02	*
439	0.1076	111526.61	+540823.6	15.077	0.065	14.348	0.091	13.966	0.071	0.01	
440	0.2642	111907.01	+600430.8	16.153	0.089	15.217	0.106	14.455	0.079	0.01	
441	0.2036	111943.37	+451612.7	16.296	0.102	15.294	0.083	14.194	0.065	0.01	*
442	0.1587	112027.49	+585613.5	15.709	0.079	15.006	0.102	14.500	0.087	0.01	
445	0.2424	112319.19	+362330.5	16.203	0.088	15.590	0.125	14.640	0.088	0.02	*
447	0.3097	112330.90	+310519.5	16.967	0.162	16.029	0.172	15.479	0.170	0.01	
448	0.2828	112437.41	+045618.9	16.684	0.190	15.609	0.165	15.141	0.187	0.05	
450	0.2445	112500.63	+001441.5	16.475	0.159	15.770	0.173	15.018	0.188	0.02	*
451	0.2605	112507.35	+023719.1	16.523	0.146	15.708	0.174	14.685	0.128	0.03	*
456	0.2041	112832.70	+414413.8	16.027	0.089	15.212	0.094	14.227	0.065	0.01	*
457	0.2689	112838.77	+505423.9	16.708	0.176	15.773	/	15.348	0.161	0.01	
459	0.1120	112939.87	+605742.5	14.927	0.064	14.287	0.076	13.953	0.076	0.01	
460	0.1915	112947.17	+342842.4	16.557	0.129	15.702	0.140	14.885	0.107	0.02	*
463	0.1182	113320.55	−033337.6	15.946	0.103	15.291	0.123	14.707	0.138	0.04	
465	0.2614	113417.17	+503004.4	16.027	0.102	15.256	0.102	14.438	0.087	0.01	*
466	0.1741	113541.21	+592748.3	15.583	0.077	15.181	0.112	14.281	0.082	0.01	*
469	0.1112	113721.36	+612001.1	15.424	0.066	14.834	0.095	14.332	0.075	0.03	
470	0.1836	113742.75	+395946.4	16.182	0.099	15.364	0.108	14.679	0.086	0.01	
471	0.2064	114113.39	+342744.3	16.115	0.096	15.778	0.158	14.823	0.116	0.02	*
472	0.1245	114132.98	−030231.5	15.697	0.079	14.966	0.090	14.369	0.102	0.02	
474	0.2011	114245.13	+620719.1	16.680	0.134	15.858	0.149	15.375	0.184	0.02	
475	0.2226	114258.39	+102747.9	16.373	0.156	15.089	/	14.401	/	0.06	
476	0.1738	114348.83	+571845.4	15.902	0.080	15.301	0.086	14.572	0.071	0.01	*
478	0.1283	114544.97	+024127.2	15.760	0.110	15.129	0.134	14.708	0.150	0.02	
479	0.1300	114642.55	+511030.6	15.756	0.086	14.818	0.105	14.489	0.089	0.01	
481	0.1296	115026.96	+512419.8	15.722	0.079	14.969	0.104	14.354	0.080	0.01	*
482	0.1951	115138.24	+004946.6	16.421	0.165	15.691	0.184	14.906	0.149	0.02	*
483	0.1625	115206.20	+015014.2	15.713	0.123	14.955	0.123	13.985	0.094	0.01	*
484	0.0699	115245.65	+101623.8	14.910	0.079	14.303	0.100	13.729	0.075	0.03	*
487	0.0645	115326.44	+580644.7	15.116	0.077	14.487	0.075	13.974	0.066	0.02	
488	0.1467	115402.02	+613843.7	15.709	0.092	14.866	0.078	14.232	0.084	0.04	
489	0.2088	115547.65	+004851.8	16.396	0.151	15.728	0.155	14.735	0.127	0.01	*
493	0.1282	115759.51	+370738.2	15.458	0.072	14.725	0.070	14.168	0.078	0.01	
494	0.1716	115843.42	+650828.6	16.489	0.148	15.647	0.142	14.854	0.132	0.01	*

Table 1 – *continued*

No. Name	Z	RA (2000, 2MASS)	Dec.	J	J_e	H	H_e	K	K_e	E(B − V)	Note
495	0.4967	120001.64	+073235.2	17.385	/	15.738	/	14.997	0.144	0.01	
496	0.1156	120041.39	+314746.2	15.545	0.066	14.937	0.081	14.304	0.074	0.02	*
497	0.1354	120324.94	+044649.9	16.112	0.136	15.311	0.125	14.451	0.093	0.01	*
500	0.1902	120739.41	+022854.6	16.193	0.123	15.833	0.176	15.000	0.144	0.01	*
501	0.1855	121126.82	−030902.7	16.040	0.095	15.177	0.105	14.704	0.112	0.03	
502	0.1931	121416.40	+371315.7	16.442	0.140	15.807	0.164	15.083	0.136	0.02	*
505	0.2132	121835.43	+022239.9	16.253	0.104	15.674	0.146	14.978	0.164	0.02	*
506	0.0939	121839.41	+470627.7	15.469	0.070	14.889	0.091	14.086	0.060	0.01	*
507	0.1992	121849.88	+502617.8	16.123	0.095	15.364	0.106	14.681	0.089	0.02	*
509	0.4747	121915.19	+410849.3	16.814	0.154	16.140	0.200	15.617	0.181	0.02	
510	0.1183	122012.64	−010531.6	16.464	0.130	15.827	0.122	15.394	0.213	0.03	
511	0.1246	122012.86	+044017.1	15.524	0.081	14.797	0.088	14.125	0.088	0.01	
512	0.2029	122024.31	+490427.3	16.297	0.132	15.977	0.211	15.112	0.172	0.01	*
513	0.1680	122031.04	+520851.2	16.115	0.113	15.374	0.137	14.631	0.119	0.02	*
514	0.2670	122121.52	+014018.1	16.550	0.181	15.780	0.168	14.404	/	0.02	
515	0.1728	122217.85	−000743.7	15.920	0.113	14.991	0.102	13.602	0.068	0.02	*
516	0.1393	122341.47	+080651.3	16.299	0.115	15.703	0.147	14.653	0.104	0.02	*
517	0.1987	122357.36	−023312.9	16.398	0.154	15.349	0.097	14.556	0.111	0.03	
518	0.1256	122443.41	+442438.9	14.894	0.056	14.233	0.075	13.439	0.051	0.01	*
519	0.1556	122505.32	+160701.5	16.459	0.144	16.147	/	15.160	0.135	0.02	
520	0.2071	122552.49	+430224.8	16.440	0.126	16.089	0.206	15.670	0.213	0.02	*
521	0.1945	122709.85	+124854.6	16.181	0.113	15.310	0.109	14.726	0.086	0.02	
524	0.1307	122814.89	+492935.3	16.486	0.134	15.739	0.143	15.110	0.146	0.01	
527	0.2210	122920.59	+415816.9	16.578	0.159	15.659	0.145	15.185	0.198	0.02	
528	0.1024	122930.40	+384620.9	15.791	0.102	15.085	0.115	14.284	0.086	0.01	*
532	0.4364	123231.81	+403124.7	17.166	0.214	16.438	0.233	15.902	0.212	0.02	
533	0.4135	123309.90	+154952.4	17.463	0.238	16.383	/	15.277	0.106	0.02	
534	0.1909	123430.24	+410934.9	16.232	0.106	15.575	0.134	14.984	0.114	0.02	*
536	0.2267	123503.45	+505049.7	16.724	0.191	15.367	/	15.117	0.143	0.01	
537	0.1393	123658.80	+261619.4	16.055	0.090	15.175	0.095	14.424	0.058	0.01	
539	0.1796	123804.93	+670320.4	16.608	0.168	15.044	/	14.245	/	0.01	
540	0.0829	123843.43	+092736.5	14.564	0.064	13.880	0.086	13.298	0.059	0.01	*
541	0.1605	124037.81	+353437.4	15.955	0.097	15.588	0.129	14.631	0.120	0.01	*
542	0.1353	124136.22	+614043.5	15.331	0.067	14.623	0.092	13.684	0.056	0.01	*
544	0.2814	124337.36	−023200.0	16.631	0.131	15.917	0.137	15.178	0.159	0.02	*
545	0.1071	124406.61	+652925.2	15.410	0.066	14.374	0.085	13.637	0.057	0.01	
546	0.2439	124428.70	+435628.7	17.203	0.235	16.014	0.162	15.329	0.155	0.01	
550	0.2224	124750.26	+052200.0	16.367	0.117	15.649	0.126	14.886	/	0.02	
553	0.2284	124855.04	+444213.4	16.367	0.158	15.923	0.210	15.071	0.151	0.02	*
555	0.2389	125334.49	−034158.1	16.591	0.150	15.761	0.167	14.694	0.112	0.02	*
557	0.1642	125503.63	+012233.7	16.307	0.130	15.756	0.168	14.843	0.159	0.01	*
560	0.2256	125708.53	+333454.2	16.966	0.209	15.954	0.206	15.493	0.173	0.01	
562	0.0552	125850.80	+523913.3	14.670	0.075	14.069	0.106	13.580	0.065	0.01	
563	0.1834	125858.09	+575022.3	15.803	0.089	15.138	0.112	14.618	0.117	0.01	
/ 2MASS 130005	0.080	130005.35	+163214.9	14.035	0.039	13.016	0.037	11.870	0.025	0.02	* (9)
564	0.0883	130038.10	+545436.8	15.460	0.074	14.736	0.089	14.118	0.087	0.01	
566	0.1379	130600.68	+000125.1	16.349	0.114	15.492	0.115	14.689	0.104	0.02	*
569	0.2403	130906.57	+481829.0	16.159	0.116	15.596	0.141	14.570	/	0.01	
570	0.1439	130942.69	+014852.1	15.824	0.103	15.301	0.125	14.471	0.107	0.03	*
571	0.2398	131104.66	+272807.3	16.017	0.109	15.148	0.100	14.534	0.122	0.01	
572	0.2032	131130.20	+555849.3	16.751	0.177	15.865	0.183	14.826	0.131	0.01	*
576	0.5847	131327.45	+145338.7	16.781	0.153	15.585	0.109	14.478	0.062	0.02	*
577	0.1610	131634.56	+632430.6	16.485	0.148	15.715	0.153	15.084	0.149	0.01	*
578	0.0906	131639.76	+445234.9	14.508	0.056	13.245	0.044	11.878	0.028	0.01	*
579	0.1569	131836.67	+580838.5	16.084	0.090	15.246	0.083	14.655	0.068	0.01	
581	0.2825	131916.82	+123221.4	16.210	0.101	15.485	0.111	14.828	0.111	0.03	*
582	0.2235	132029.12	+662333.2	16.148	0.102	15.317	0.114	14.459	0.099	0.02	*
583	0.2026	132156.76	+114147.0	16.425	0.151	15.815	0.168	15.199	0.197	0.02	*
/ IRAS 13197−1627	0.017	132224.47	−164342.4	12.341	0.078	11.568	0.094	10.877	0.050	0.09	(10)
586	0.0713	132345.99	+610400.1	15.315	0.095	14.665	0.123	13.898	0.073	0.01	*
587	0.2027	132419.89	+053704.6	15.753	0.095	14.208	0.051	12.070	0.024	0.03	*
588	0.1445	132420.09	+634059.9	16.214	0.111	15.843	0.162	15.133	0.126	0.01	*
590	0.4290	132529.29	+592425.0	16.353	0.128	15.592	0.131	14.880	0.115	0.01	*
591	0.2118	132553.80	+405852.2	16.150	0.104	15.563	0.137	14.862	0.106	0.01	*

Table 1 – *continued*

No. Name	Z	RA (2000, 2MASS)	Dec.	J	J_e	H	H_e	K	K_e	E(B − V)	Note
592	0.2229	132658.91	+262806.3	15.803	0.082	14.970	0.081	14.557	0.100	0.01	
595	0.2842	133332.04	+300745.0	16.630	0.144	15.819	0.160	14.997	0.114	0.01	*
597	0.1694	133542.44	+631641.3	16.262	0.106	15.540	0.131	14.881	0.102	0.01	*
600	0.3292	133735.02	−012815.5	16.422	0.143	15.868	0.174	14.972	0.172	0.02	*
601	0.2922	133827.08	+552701.8	16.715	0.155	16.114	0.194	15.038	0.124	0.01	*
602	0.1382	134017.79	+551807.3	15.433	0.066	14.708	0.077	14.128	0.063	0.01	
604	0.1938	134317.94	+394737.8	16.322	0.086	15.852	0.121	14.947	0.094	0.01	*
605	0.2759	134418.64	+053626.2	17.050	0.211	15.954	0.202	15.114	0.175	0.02	
608	0.1798	134602.87	+001650.3	16.494	0.156	16.005	0.176	15.376	0.212	0.02	*
609	0.1204	134733.41	+121724.1	14.933	0.071	14.191	0.081	13.216	0.051	0.03	*
610	0.1563	134735.65	+631400.1	15.540	0.074	14.820	0.096	14.351	0.089	0.02	
/ A1795_1	1.99	134849.5	+263711#	22.43	0.23	21.13	0.13	19.00	0.13	0.01	* (6)(9),*JHK*(9)
/ A1795_2	1.30	134906.4	+263748#	18.76	0.05	17.98	0.05	17.01	0.05	0.01	* (6)(9),*JHK*(9)
613	0.2295	135046.63	+081527.6	16.310	0.135	15.729	0.138	14.938	0.147	0.02	*
615	0.2833	135122.71	+420652.9	16.487	0.123	15.732	0.159	15.001	0.135	0.01	*
616	0.2409	135239.96	+030802.3	15.792	0.079	15.084	0.078	14.423	0.101	0.02	*
617	0.2063	135251.16	+654113.2	15.792	0.082	15.354	0.103	14.374	0.071	0.01	*
618	0.1662	135347.69	+425831.5	16.046	0.113	15.660	0.176	14.824	0.123	0.01	*
619	0.3755	135400.37	+520151.3	16.942	0.221	15.938	0.214	15.582	0.287	0.01	
620	0.1344	135617.79	−023101.4	16.218	0.131	15.234	0.159	14.603	0.110	0.04	
621	0.1731	135621.86	+013223.7	15.983	0.104	15.182	0.085	14.532	0.096	0.03	
623	0.1232	135646.10	+102608.7	15.161	0.084	14.470	0.095	13.982	0.083	0.03	
624	0.1949	135650.34	+425320.5	16.068	0.097	15.454	0.127	14.598	0.098	0.01	*
625	0.1948	135654.26	+425916.8	15.957	0.082	15.492	0.117	14.666	0.092	0.01	*
627	0.1314	135822.78	+474102.7	14.853	0.060	14.093	0.071	13.468	0.050	0.01	
628	0.1623	140113.84	+622610.8	16.392	0.119	15.687	0.150	15.052	0.147	0.02	*
630	0.1797	140231.57	+021546.4	15.613	0.090	14.961	0.128	14.318	0.087	0.03	*
631	0.0806	140541.23	+402632.5	15.097	0.042	14.608	0.056	13.926	0.051	0.01	*
632	0.1706	140712.94	+585120.5	16.052	0.092	15.358	0.119	14.712	0.102	0.01	*
634	0.2413	140842.42	+043051.4	16.359	0.156	15.528	0.148	14.989	0.156	0.02	
635	0.1654	140845.72	+353218.5	15.271	0.063	14.526	0.067	13.993	0.056	0.01	
637	0.1816	140857.48	+035533.6	15.919	0.109	15.690	0.190	14.948	0.169	0.02	*
638	0.4617	141120.47	+521209.6	16.778	0.176	15.178	/	15.367	0.187	0.01	
639	0.1820	141243.00	+094820.8	16.323	0.137	15.565	0.124	14.966	0.161	0.02	
642	0.1308	141416.95	+050417.8	16.372	0.184	15.317	0.175	15.288	0.212	0.02	
643	0.1156	141441.59	−024950.7	15.329	0.075	14.574	0.080	13.788	0.061	0.06	*
644	0.1478	141525.74	−011352.7	15.635	0.102	15.059	0.109	14.368	0.094	0.04	*
645	0.2116	141705.53	+321239.3	16.052	0.088	15.302	0.101	14.664	0.097	0.01	
647	0.2326	142209.93	+250927.6	16.325	0.115	15.614	0.136	14.830	0.099	0.01	*
649	0.1328	142314.45	+635804.1	15.488	0.075	14.862	0.087	14.234	0.076	0.01	*
651	0.2429	142805.32	+534542.0	16.134	0.102	15.408	0.122	14.667	0.114	0.01	*
653	0.3177	143027.66	−005614.7	16.500	0.155	15.993	0.197	14.823	0.158	0.03	*
654	0.0851	143029.89	+133912.1	14.322	0.040	13.786	0.050	13.171	0.047	0.02	*
657	0.1381	143237.25	+012050.8	15.887	0.087	15.211	0.123	14.448	0.079	0.04	*
658	0.2002	143238.63	+051921.8	15.801	0.083	14.936	0.078	13.956	0.052	0.03	*
659	0.2525	143314.09	+094551.3	16.836	0.207	15.858	0.158	14.978	0.145	0.02	*
661	0.3406	143412.08	+321102.6	16.529	0.148	15.965	0.204	15.413	0.174	0.01	*
662	0.2470	143450.26	+463302.8	16.527	0.124	15.991	0.199	15.033	0.134	0.01	*
663	0.1441	143552.63	+553139.0	15.902	0.127	15.240	0.111	14.705	0.089	0.01	
664	0.1280	143607.23	+492858.5	15.539	0.084	14.872	0.103	14.284	0.086	0.03	*
665	0.2169	143728.27	+514545.2	16.289	0.134	15.492	0.144	15.157	0.178	0.01	
666	0.0922	143737.84	+301101.3	14.755	0.058	13.946	0.073	13.516	0.058	0.01	
668	0.0370	144038.10	+533016.0	14.006	0.047	13.270	0.057	12.651	0.047	0.01	
669	0.3579	144114.21	+503008.7	16.559	0.153	16.026	0.182	15.183	0.200	0.02	*
670	0.2202	144157.26	+094859.1	16.385	0.157	15.657	0.160	14.740	0.136	0.02	*
671	0.2685	144239.83	+421141.0	16.318	0.121	15.480	0.122	14.826	0.121	0.01	
673	0.1312	144541.31	+334107.8	15.720	0.067	15.017	0.068	14.398	0.077	0.01	*
676	0.2938	144815.27	+391327.1	16.963	0.202	15.667	0.152	15.294	/	0.01	
678	0.1784	144920.70	+422101.5	15.717	0.076	14.623	0.066	13.095	0.037	0.01	*
679	0.1194	145019.18	−010647.6	15.631	0.105	15.062	0.115	14.288	0.099	0.04	*
680	0.2673	145134.69	+014711.6	17.243	0.221	16.298	0.215	15.369	0.191	0.04	*
682	0.0873	145519.42	+322601.7	15.564	0.076	14.745	0.082	14.479	0.086	0.01	
683	0.1834	145544.78	+605951.4	15.910	0.087	15.264	0.096	14.498	0.081	0.01	*
684	0.2467	145549.48	+485436.0	16.701	0.180	15.526	0.171	14.724	0.136	0.02	

Table 1 – *continued*

No. Name	Z	RA (2000, 2MASS)	Dec.	J	J_e	H	H_e	K	K_e	$E(B-V)$	Note
686	0.1519	145721.66	+592944.2	15.691	0.077	14.896	0.088	14.172	0.078	0.01	*
688	0.3386	150117.94	+545517.9	16.153	0.102	15.436	0.138	14.556	0.093	0.01	*
689	0.1640	150134.76	+544733.8	16.297	0.162	14.451	/	14.842	0.122	0.01	
692	0.2355	150217.26	+380306.9	16.872	0.201	15.174	/	15.149	0.177	0.01	
694	0.1826	150420.91	+015159.5	15.455	0.071	14.672	0.064	13.746	0.068	0.05	*
695	0.2282	150425.13	+390828.8	15.833	0.087	15.067	0.093	14.470	0.103	0.01	
696	0.2829	150434.97	+354551.9	16.796	0.141	16.172	0.177	15.364	0.161	0.01	*
698	0.2506	150625.09	+401353.9	16.738	0.174	15.810	0.167	15.141	0.178	0.01	
699	0.1819	150719.93	+002905.1	15.836	/	15.464	0.111	13.990	/	0.06	
701	0.1114	150904.21	+043441.7	15.676	0.095	14.835	0.071	14.160	0.084	0.04	
706	0.1460	151247.15	−014423.4	16.485	0.111	15.738	0.128	14.991	0.148	0.15	*
707	0.2077	151315.08	+431959.9	15.865	0.099	15.307	0.128	14.564	0.122	0.01	*
709	0.1353	151709.24	+335324.5	15.209	0.056	14.414	0.058	13.984	0.058	0.02	
711	0.1378	151907.37	+520605.9	14.757	0.050	13.631	0.050	12.461	0.031	0.02	*
712	0.1996	151933.76	+340635.4	16.282	0.112	15.475	0.115	14.765	0.131	0.01	
713	0.1887	152223.57	+435051.6	16.223	0.099	15.452	0.089	14.562	0.098	0.02	*
715	0.2255	152428.86	+400759.9	16.440	0.131	15.525	0.145	14.886	0.152	0.02	
717	0.3450	153031.16	+424657.0	16.906	0.146	16.582	0.245	15.086	0.148	0.03	*
720	0.1985	153204.81	+475025.1	15.930	0.080	15.479	0.100	14.598	0.104	0.01	*
722	0.1286	153338.03	+355708.2	16.263	0.112	15.608	0.148	14.994	0.128	0.02	
723	0.1738	153401.63	+025217.9	16.183	0.139	15.244	0.127	14.314	0.102	0.04	*
724	0.2056	153431.03	+031527.7	15.641	0.089	14.775	0.075	14.082	0.093	0.04	
726	0.1532	153647.54	+373712.4	16.149	0.093	15.672	0.105	14.785	0.092	0.01	*
734	0.3105	154337.84	−004419.5	16.597	0.147	15.845	0.178	14.937	0.146	0.09	*
737	0.2347	154413.75	+370235.7	16.338	0.128	15.744	0.153	14.909	0.107	0.01	*
738	0.3177	154623.80	+360629.7	15.962	/	15.057	/	15.344	0.170	0.02	
739	0.2128	154728.34	+491202.8	16.136	0.110	15.497	0.127	14.800	0.128	0.01	*
741	0.1215	154832.37	−010811.8	16.351	0.111	15.913	0.168	15.111	0.185	0.11	*
742	0.1430	155020.02	+243238.7	16.682	0.190	16.020	0.214	15.119	0.137	0.04	*
744	0.0745	155225.67	+275343.4	14.691	0.053	14.127	0.069	13.576	0.058	0.03	*
745	0.1968	155315.94	+440749.3	15.910	0.085	15.113	0.085	14.168	0.077	0.03	*
746	0.1517	155443.61	+340228.4	15.631	0.077	14.956	0.103	14.574	0.100	0.02	
747	0.1493	155522.05	+281323.1	15.639	0.075	14.793	0.071	14.198	0.083	0.03	
748	0.1870	155524.56	+413016.5	16.205	0.116	15.556	0.147	14.691	0.097	0.01	*
750	0.1195	155829.36	+351328.5	16.157	0.101	15.461	0.118	14.909	0.103	0.02	
751	0.2181	155930.39	+380838.9	16.566	0.136	15.550	0.127	14.924	0.109	0.01	
752	0.1894	160028.31	+512812.3	16.570	0.140	15.358	/	15.222	0.182	0.01	
754	0.3604	160219.50	+071329.0	16.665	0.172	16.238	/	15.405	0.199	0.04	
756	0.1584	160631.38	+273643.5	16.396	0.102	15.784	0.135	15.312	0.193	0.04	
759	0.2335	161259.83	+421940.5	16.567	0.150	16.047	0.221	14.685	0.115	0.01	*
760	0.1531	161318.80	+305436.9	15.812	0.090	15.260	0.101	14.499	0.088	0.03	*
761	0.1531	161325.56	+460033.7	15.653	0.071	14.853	0.087	14.404	0.092	0.01	
766	0.1519	161647.31	+371621.3	15.365	0.066	14.616	0.064	14.081	0.070	0.01	
767	0.1863	161655.00	+432130.8	16.390	0.115	15.888	0.180	14.867	0.140	0.01	*
771	0.1321	162103.43	+402500.5	15.719	0.082	15.079	0.107	14.578	0.095	0.01	
773	0.2661	162209.42	+352107.2	16.936	0.145	16.113	0.178	14.929	0.103	0.01	*
774	0.1224	162436.42	+334406.7	16.045	0.099	15.342	0.107	14.688	0.095	0.02	*
776	0.4237	162516.88	+265233.8	17.167	0.233	16.222	0.220	15.155	0.135	0.03	*
/ A2199_2	2.83	162810.1	+393513#	21.09	0.08	21.15	0.16	20.27	0.12	0.01	* (6),*JHK*(6)
778	0.1818	162833.41	+354708.2	15.544	0.062	14.720	0.065	13.977	0.051	0.01	
780	0.2228	163150.36	+445355.5	15.937	0.086	15.261	0.116	14.690	0.084	0.01	
781	0.1748	163345.01	+372335.2	16.108	0.089	15.425	0.115	14.775	0.124	0.01	*
782	0.2156	163419.19	+464801.5	16.369	0.121	15.427	0.144	15.235	0.189	0.02	
788	0.1512	164019.68	+403744.4	16.497	0.133	15.493	0.133	14.787	0.112	0.01	
887	0.2210	164126.90	+432121.6	16.901	0.173	15.904	0.179	14.732	0.124	0.01	*
791	0.2013	164224.46	+372844.6	16.406	0.123	15.768	0.148	15.028	0.145	0.01	*
792	0.1468	164232.19	+431417.3	16.140	0.088	15.542	0.122	15.168	0.177	0.01	
795	0.1312	164435.38	+420029.9	15.933	0.091	15.258	0.125	14.474	0.095	0.01	*
796	0.1217	164716.66	+384327.7	15.866	0.091	15.332	0.124	14.635	0.106	0.01	*
797	0.1034	165315.06	+234942.8	15.133	0.055	14.331	0.051	13.927	0.065	0.05	
799	0.1890	170050.21	+195143.1	16.211	0.119	15.787	0.153	14.827	0.102	0.07	*
800	0.2097	170120.68	+215231.4	15.413	/	14.640	/	14.647	0.108	0.06	
803	0.1942	171139.83	+315248.6	16.065	0.083	15.335	0.096	14.652	0.082	0.04	*
804	0.1050	171245.93	+291715.3	15.813	0.081	15.080	0.083	14.411	0.080	0.04	*

Table 1 – *continued*

No. Name	Z	RA (2000, 2MASS)	Dec.	J	J_e	H	H_e	K	K_e	E(B − V)	Note
805	0.1128	171350.33	+572954.9	15.349	0.064	14.604	0.072	13.892	0.065	0.02	∗
/ AMS 09	2.1	171435.64	+585652.4	16.426	0.141	15.795	0.162	14.639	/	0.02	(10)
806	0.1568	171544.01	+600835.2	15.972	0.087	15.194	0.111	14.684	0.114	0.02	
807	0.5235	171559.77	+280716.9	17.150	0.206	15.755	0.121	14.630	0.084	0.05	∗
/ 2MASS 191105	0.171	191105.53	+674250.7	17.755	/	15.683	0.143	14.483	0.107	0.02	(20)
813	0.1252	205436.70	−053700.1	16.353	0.141	14.863	/	14.906	0.122	0.05	
815	0.1769	205610.42	−063037.8	16.119	0.118	15.389	0.143	14.881	0.144	0.05	
817	0.2064	205840.00	+003931.0	16.125	0.084	15.112	0.080	14.473	0.087	0.07	
819	0.2349	212653.81	+003553.0	16.430	0.124	15.798	0.156	14.998	0.138	0.04	∗
820	0.1261	213340.87	+100929.0	15.415	0.084	14.722	0.097	14.254	0.093	0.04	
821	0.0886	213400.60	−074942.9	15.583	0.084	15.007	0.098	14.512	0.095	0.03	
822	0.3061	213446.01	−002707.4	16.738	0.171	15.932	0.253	14.715	0.121	0.06	∗
/ MS 2137_4	3.33	213952.4	−233737#	21.55	0.12	20.02	0.07	19.02	0.05	0.05	(6),*JHK*(6)
823	0.1684	214247.89	+000156.4	16.719	0.149	15.894	0.176	15.191	0.148	0.06	
824	0.1576	214425.53	−081029.5	16.570	0.148	15.868	0.187	14.871	/	0.05	
827	0.1092	215425.75	+113129.5	15.475	0.072	14.746	0.079	14.157	0.089	0.07	
/ A2390_12	2.28	215329.0	+174854#	19.48	0.05	18.35	0.03	17.70	0.03	0.06	(6),*JHK*(6)
/ A2390_15	2.78	215333.2	+174210#	/	/	20.07	0.06	18.83	0.04	0.06	(6),*JHK*(6)
/ A2390_18	1.467	215334.0	+174241#	18.65	0.03	17.57	0.02	16.49	0.02	0.06	∗ (6)(11),*JHK*(6)
882	0.3903	215731.41	+003756.7	16.715	/	15.518	/	15.135	0.142	0.05	
829	0.1932	215923.86	−010631.0	16.600	0.135	15.918	0.246	14.902	0.132	0.09	∗
/ 2MASS 220906	0.425	220906.02	−325750.5	16.701	0.146	15.778	0.122	15.134	0.160	0.04	(20)
832	0.1805	221217.94	−094407.6	16.173	0.111	15.371	0.133	14.575	0.104	0.04	∗
833	0.2176	222246.97	+133941.0	16.412	0.128	15.468	0.122	14.795	0.144	0.07	
837	0.2344	222604.05	−084841.8	16.538	0.141	15.537	0.147	14.947	0.156	0.04	
840	0.1971	223854.79	−002826.8	16.327	0.112	15.491	0.137	14.703	0.108	0.06	∗
848	0.1493	225510.12	−081234.3	16.422	0.134	15.567	0.172	14.301	/	0.04	
850	0.2335	225832.12	+010836.4	16.726	0.160	14.957	/	15.360	0.174	0.06	
851	0.1811	230007.93	−082019.9	16.235	0.159	15.425	0.138	14.601	0.129	0.04	∗
853	0.2266	230531.65	+151247.4	16.252	0.106	15.655	0.115	14.789	0.112	0.14	∗
854	0.2503	230612.92	−005912.4	16.859	0.186	15.921	0.180	15.016	0.128	0.05	∗
/ IRAS F23060+0505	0.174	230833.96	+052129.8	14.564	0.054	13.152	0.042	11.644	0.029	0.04	∗ (14)
856	0.2223	231602.96	−103615.1	16.523	0.135	15.130	/	14.780	0.135	0.03	
858	0.2185	233220.83	+152915.4	16.660	0.155	15.759	0.137	15.246	0.198	0.06	
859	0.1698	233313.16	+004911.7	16.033	0.090	14.830	0.084	13.625	0.045	0.03	∗
860	0.2431	233603.75	−104639.9	16.282	0.110	15.847	0.168	14.901	0.148	0.02	∗
876	0.6277	235831.04	−002228.6	16.793	0.131	16.048	0.159	15.727	0.200	0.03	

Note. The symbol '#' after the coordinate indicates the coordinate from the original reference.
Note the symbol '∗' in the note indicates the source located near the power-law distribution in Fig. 1.
Note for references: (1) Zakamska et al. (2003); (2) Vignali et al. (2006); (3) Vignali, Alexander & Comastri (2004) (4) Norman et al. (2002); (5) Derry et al. (2003); (6) Gandhi et al. (2004); (7) Beichman et al. (2003) (8) Sturm et al. (2006); (9) Schmidt et al. (2002); (10) Dadina & Cappi (2004); (11) Crawford et al. (2001) (12) Martinez-Sansigre et al. (2006); (13) Fabian et al. (2000); (14) Brandt et al. (1997) (15) Serjeant et al. (1998); (16) Soifer et al. (1991); (17) Gregg et al. (2002); (18) Glikman et al. (2004); (19) Boyle et al. (1998) and (20) Leipski et al. (2007).

$m(\lambda_1) - m(\lambda_2)$ as $J - H$ and $H - K$, respectively, the blackbody line can be determined and is shown in Fig. 1.

It is seen from Fig. 1 that majority of type II Seyfert galaxies are distributed in the region around the blackbody line that coincides with the previous result from Dultzin-Hacyan & Benitz (1994) for a small sample and is indicative of thermal radiation dominating from the starlight in the galaxy discs, because the host emissions generally dominate the nuclear emissions. As Dultzin-Hacyan & Benitz (1994) point out, the near-infrared emissions of type II Seyfert galaxies are mainly dominated by evolved massive red giants and supergiants in the galaxy discs. It is seen that almost all PG quasars are distributed in the region around the power-law line indicative of non-thermal core-dominated properties. According to the unified scheme (Antonucci 1993; Urry & Padovani 1995), it is not so hard to explain such a distribution, because for type I quasars with a small viewing angle, radiation from the central part can be directly received by observers without obstruction from the torus. For type II quasars, the distribution in Fig. 1 is somewhat puzzling. It can be seen that about 43 per cent of them are distributed in the region around the blackbody line. However, about 57 per cent of them are distributed in the region around the power-law line (those sources are indicated with the symbol '*' in the note of Table 1). As expected, the former group has a similar nature to type II Seyfert galaxies with a thermal radiation from starlight on the host galaxies in the near-infrared and with a large view angle, therefore radiation from the central part is mostly obscured by the torus. However, the latter group has a similar nature to PG quasars showing non-thermal dominant properties. One possibility is that for later sources the torus is not so thick and the viewing angle is not large enough so that some near-infrared radiation from the central part can still penetrate the torus. It should be pointed out that some of those sources may have hidden broad lines in the near-infrared. Direct evidence of the hidden type I nuclei for type II quasars comes from Zakamska et al. (2005). They found that broad emission lines were detected for several type II quasars in spectropolarimetric observations. In addition, there is also

Table 2. *IRAS* Observation of type II quasars.

No. Name	Z	*IRAS*	F25	F60	F100
20	0.1175	F00402+1516	/	0.587	0.789
/ 2MASS 044114	0.236	F04394−3740	0.173	0.823	1.191
151	0.0544	F07559+5058	0.359	0.708	0.786
157	0.2384	F07592+3736	/	0.285	0.663
158	0.0811	F07598+2601	0.296	0.514	/
164	0.1284	F08023+2826	/	0.277	/
177	0.1244	F08112+3039	/	0.233	/
191	0.1546	F08275+3719	/	0.427	/
200	0.1170	F08317+5251	0.089	0.313	/
245	0.2604	F08507+3636	/	0.250	/
249	0.2006	F08516+5032	/	0.225	/
261	0.3291	F09005+0223	/	0.363	/
268	0.3407	F09036+2706	/	0.197	/
281	0.4409	F09105+4108	0.333	0.525	/
297	0.5308	F09220+2759	/	0.301	/
321	0.1280	F09425+1751	0.436	0.889	0.569
337	0.1481	F09575+1256	/	0.283	/
346	0.1204	F10034+0726	/	0.813	0.972
351	0.0977	F10080+0626	0.288	0.519	0.594
377	0.0511	F10308+6017	0.464	0.809	0.796
387	0.4860	F10372+4801	/	0.219	/
416	0.0776	F10590+6515	0.217	0.541	0.953
423	0.1511	F11041+2558	/	0.221	/
428	0.1815	F11062+0715	/	0.399	0.906
431	0.2612	F11070+4249	/	0.469	0.583
434	0.0904	F11084−0037	/	0.704	0.961
440	0.2642	F11162+6020	/	0.675	1.110
441	0.2036	F11169+4532	/	0.211	/
445	0.2424	F11206+3639	/	0.485	0.846
456	0.2041	F11258+4201	/	0.203	/
470	0.1836	F11350+4016	/	0.195	/
488	0.1467	F11513+6155	0.147	0.279	/
542	0.1353	F12393+6157	0.128	0.711	/
545	0.1071	F12420+6545	0.117	0.399	0.561
553	0.2284	F12465+4458	/	0.209	/
566	0.1379	F13034+0017	/	0.633	0.685
578	0.0906	F13144+4508	0.508	0.674	0.877
/ IRAS 13197−1627	0.017	F13197−1627	2.855	5.895	5.476
587	0.2027	F13218+0552	0.482	1.250	/
609	0.1204	F13451+1232	0.669	1.920	2.061
623	0.1232	F13542+1040	0.212	0.797	0.605
631	0.0806	F14036+4040	0.191	0.265	/
654	0.0851	F14281+1352	0.191	0.262	/
657	0.1381	F14300+0134	/	0.227	/
666	0.0922	F14354+3024	/	0.236	/
668	0.0370	F14390+5343	0.509	1.311	1.852
678	0.1784	F14474+4233	0.234	0.403	/
684	0.2467	F14541+4906	0.200	0.530	0.543
689	0.1640	F15001+5459	/	0.142	/
701	0.1114	F15065+0446	0.119	0.338	/
709	0.1353	F15151+3404	/	0.151	/
711	0.1378	F15176+5216	0.279	0.780	1.342
/ IRAS F15307+3252	0.926	F15307+3252	0.071	0.234	/
724	0.2056	F15320+0325	/	0.329	0.763
745	0.1968	F15515+4416	/	0.152	/
751	0.2181	F15577+3816	/	0.447	0.561
760	0.1531	F16113+3102	/	0.529	/
766	0.1519	F16149+3723	0.104	0.181	/
778	0.1818	F16267+3553	0.089	0.243	/
780	0.2228	F16303+4500	/	0.173	/
796	0.1217	F16455+3848	0.068	0.269	/
797	0.1034	F16511+2354	/	0.511	/
805	0.1128	F17130+5733	0.120	0.156	/
827	0.1092	F21519+1117	/	0.283	/
/ IRAS F23060+0505	0.174	F23060+0505	0.426	1.152	0.833

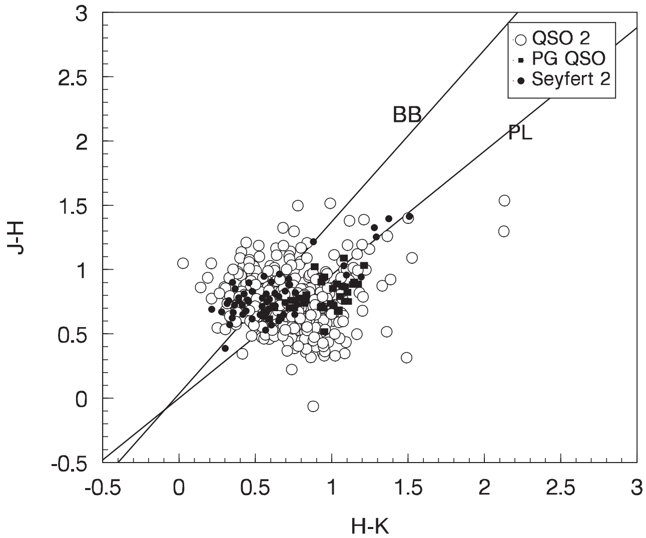

Figure 1. $(J - H) - (H - K)$ diagram for type II quasars. 'BB' and 'PL' indicate the blackbody line and the power-law line, respectively.

evidence for some type II galaxies harboring central regions similar to those of type I galaxies. The early results were from Veilleux, Sanders & Kim (1997, 1999) for ultraluminous infrared galaxies (ULIRGs) with type II Seyfert galaxy spectra. Their results show that some ULIRGs with type II Seyfert galaxy spectra have hidden broad lines, in particular, broad Pa $\alpha\,\lambda$ 1.8751 μm and [Si VI] λ1.962 μm features in the near-infrared, indicative that an important fraction of the bolometric luminosity is powered by the same mechanism as that in type I Seyfert galaxies and type I quasars, but broad lines in the optical are totally obscured by the torus. However, it was shown by Tran (2001) that in the CfA and 12 μm samples of type II Seyfert galaxies there are two intrinsically different populations of type II Seyfert galaxies: one harboring energetic, hidden type I Seyfert galaxy nuclei with broad-line regions (BLRs) and the other are pure type II Seyfert galaxies without broad lines (see also a recent example by Bianchi et al. 2008). Tran (2001) found that in the 12 μm sample about 50 per cent of type II Seyfert galaxies show polarized BLRs. Gu & Huang (2003) and Gu et al. (2006) also found some type II Seyfert galaxies with detected polarized BLRs, and suggested that those sources have powerful active galactic nucleus activity, most likely caused by high accretion rates. Recently, Gonzalez-Martin et al. (2006) pointed out that even for low-ionization nuclear emission-line regions, a true active galactic nucleus (compact non-thermal) emission from the nucleus is found from X-ray studies for about 60 per cent of the sources. Furthermore, Krongold & Dultzin-Hacyan (2002) and Koulouridis et al. (2006a, 2008) also discussed the environment of type I and II Seyfert and bright *IRAS* galaxies, and argued that while the large-scale environment difference for those sources cannot be attributed to differences in nuclear activity but rather to the different morphology of their host galaxies. However, the close (<100 kpc) environment of the active galactic nucleus is different for type I and II Seyfert galaxies. In these cases, the type of activity is mostly dominated by tidal forces and the phase of the interaction (see also Dultzin et al. 2008; Storchi-Bergmann 2008). Therefore, as Tran (2001) suggested, the simple purely orientation-based unification model may not be applicable to all (Seyfert) galaxies.

More near-infrared spectroscopic and spectropolarimetric observations at the high level are needed to confirm this possibility for

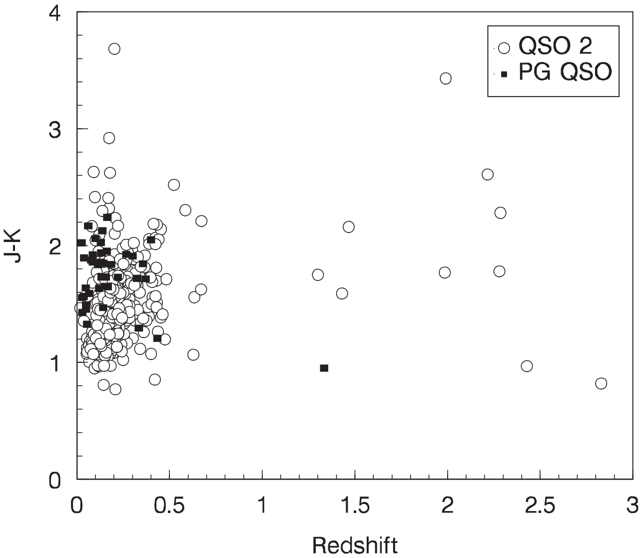

Figure 2. The relation between the near-infrared colour and the redshift for type II quasars.

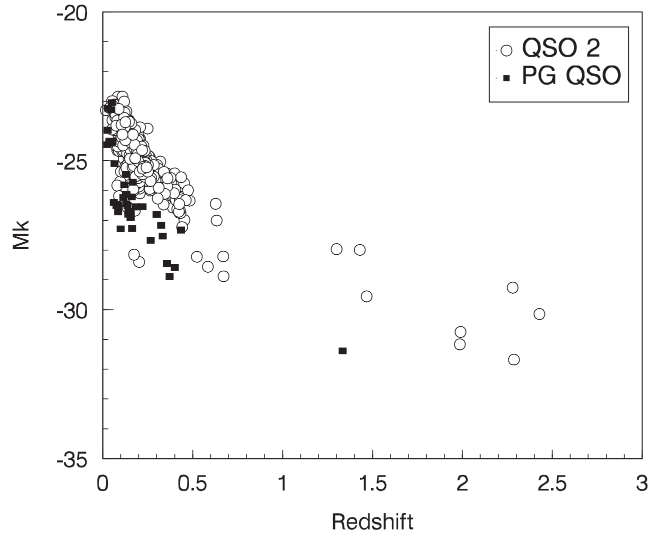

Figure 3. The relation between the absolute K magnitude and the redshift for type II quasars.

type II quasars located in the region around the power-law line in Fig. 1.

3.2 Near-infrared colour and redshift relation

Hyland & Allen (1982) indicated that, for various values of redshift from $Z = 0$ to $Z > 2.5$, the distributions of type I quasars in the near-infrared two-colour diagram strongly depend on the redshift, i.e. statistically, the sources with larger redshifts gradually occupy the region towards the lower left along with the power-law line. In order to check the status for type II quasars, taking data from Table 1 the relationship between the infrared colour ($J - K$) and the redshift Z can be shown (see in Fig. 2). About 40 type I quasars (PG quasars) selected from Schmidt & Green (1983) are also presented for comparison. However, PG quasar samples used here have redshifts less than 0.5, as shown in Fig. 2, and no clear relation between near-infrared colour and redshift is found for PG quasars in such a small redshift interval. It is seen from Fig. 2 that type II quasars are rather scatted and no clear relation between the near-infrared colour and the redshift can be seen up to $Z > 2.5$. It should be mentioned that around $Z = 2$– 2.3, the observed quasar colours exhibit a peak because Hα enters the K bandpass.

3.3 Absolute *K* magnitude with different redshifts

If the Hubble constant is taken as $H_0 = 75$ km s^{-1} Mpc^{-1} and the deceleration parameter is taken as $q_0 = 0$, then for all sources with good quality data in the K band, the luminosity distances can be obtained. The K-corrections can also be obtained with the spectral index calculations in the near-infrared. Thus, absolute magnitudes in the K band, M_{K}, can be derived for those sources. The diagram of M_{K} versus redshift is plotted in Fig. 3. For comparison, about 40 type I quasars (PG quasars) selected from Schmidt & Green (1983) are also presented. It is seen from Fig. 3 that, for either type I or II quasars (PG quasars), M_K all increase with redshift. In fact, the increase in luminosity with redshift is a reflection of the flux limit of the survey.

4 FAR-INFRARED PROPERTIES

First of all, coordinates from the original papers were used to make cross-identifications of *IRAS* counterparts in the *IRAS* Point Source Catalog (PSC) or *IRAS* Faint Source Catalog (FSC) for all type II quasars. If necessary, the coordinates given in the SIMBAD database were the references to correct source position. In this procedure, the *IRAS* positional error ellipse was used as the search criterion for each source, because the *IRAS* error ellipse has a 95 per cent confidence level (IRAS Explanatory Supplement 1988, hereafter IRAS ES). If there is more than one source within the search area, the closest one with the proper colour is selected as the counterpart. Due to the flux limit of the *IRAS* PSC or *IRAS* FSC, only 65 sources were found to have *IRAS* counterparts with data in at least one of three *IRAS* bands at 25, 60 and 100 μm, and 15 sources were found to have *IRAS* photometric data in all three *IRAS* bands. Those *IRAS* counterparts of type II quasars are listed in Table 2. The structure of Table 2 is basically the same as that for Table 1. Note that only good quality data in three *IRAS* bands are shown.

From Table 2, the typical *IRAS* two-colour diagram, [25]–[60] versus [60]–[100], is plotted in Fig. 4(a) for 15 type II quasars with good quality data (the flux density uncertainty ≤12 per cent) in all three *IRAS* bands. For comparison, *IRAS* counterparts for 60 typical type II Seyfert galaxies selected from Polletta et al. (1996) and 40 type I quasars (PG quasars) selected from Schmidt & Green (1983) were also identified. Finally, 58 type II Seyfert galaxies and 9 PG quasars were found to have good quality data at 25, 60 and 100 μm. Those type II Seyfert galaxies and PG quasars are also plotted in Fig. 4(a). In addition, according to equations (1) and (2) the power-law line and the blackbody line are also plotted in Fig. 4(a), respectively. It is seen that, as expected, PG quasars are located near the power-law line indicative of the strong non-thermal core-dominated emission while most type II Seyfert galaxies and type II quasars have a similar distribution, located between the power-law line and the blackbody line. This result may imply that, besides the influence from the core region, star formation may be stronger for type II quasars (and type II Seyfert galaxies), as pointed out by Zakamska et al. (2006) that A-type stars are an important contribution to the type II quasar hosts, and as also pointed by Verma et al. (2005) that a cooler far-infrared disc

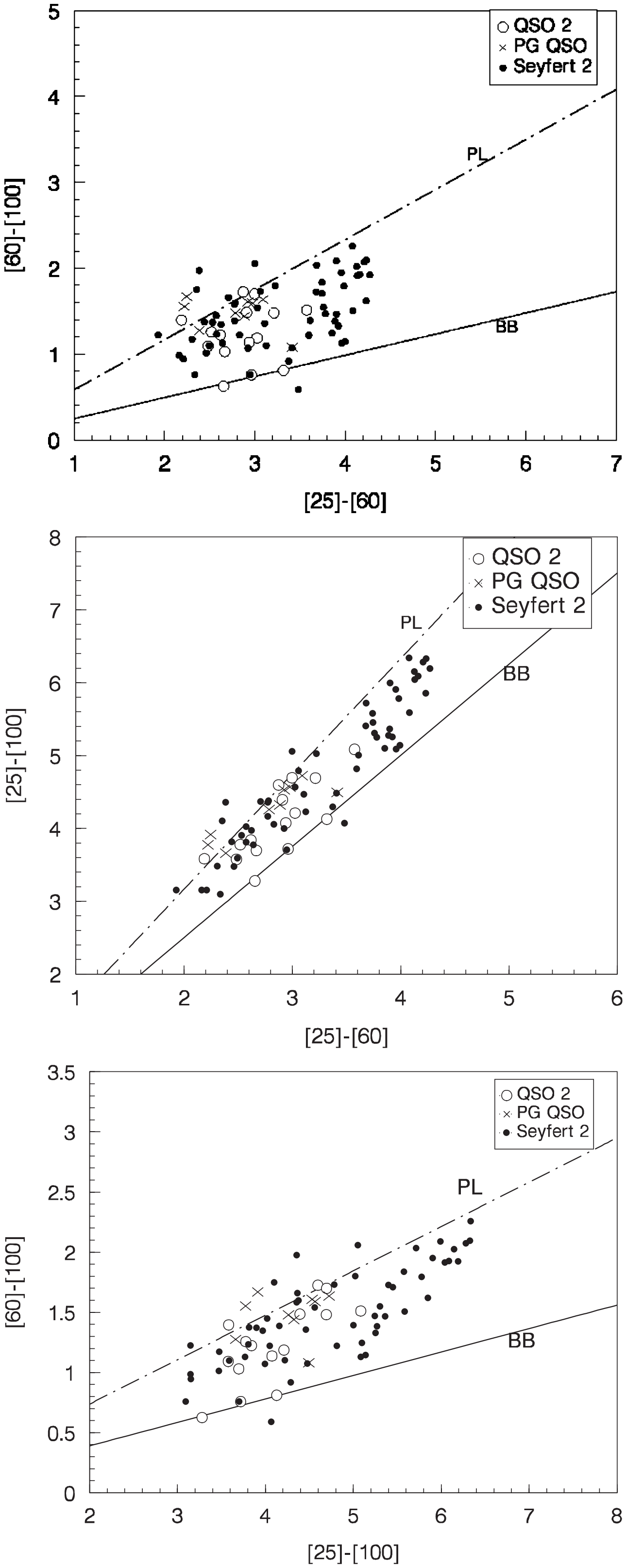

Figure 4. *IRAS* two-colour diagrams for type II quasars. 'BB' and 'PL' indicate the blackbody line and the power-law line, respectively. (a): [25]–[60] versus [60]–[100], (b): [25]–[60] versus [25]–[100] and (c): [25]–[100] versus [60]–[100].

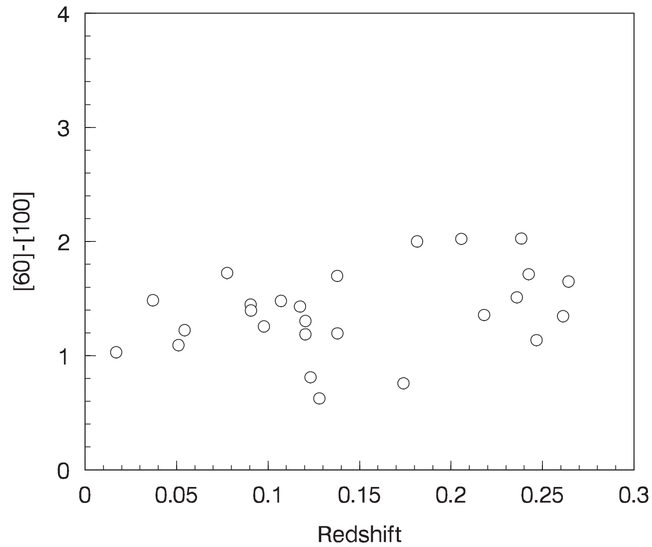

Figure 5. The relation between the far-infrared colour and the redshift for type II quasars.

component within which normal stars heat dust grains may play an important role. Another result from Fig. 4(a) is that, statistically, typical temperatures indicated by the far-infrared colours for type II Seyfert galaxies are colder than those for type II quasars. This is also a well-known result for type I sources (de Grijp, Lub & Miley 1987; de Grijp et al. 1992). In addition, Dultzin-Hacyan, Masegosa & Moles (1990) show that while the mid-infrared emission at 25 μm in type I Seyfert galaxy is synchrotron radiation (or dust re-emission of it), in type II Seyfert galaxy it is dust re-emission of starlight (see also Mouri & Taniguchi 1992; Gu et al. 1997). Furthermore, Dultzin-Hacyan, Moles & Masegosa (1988) and Dultzin-Hacyan, Masegosa & Moles (1990) found that the bulk of emission at 25 μm is of nuclear origin. The later is deduced from its correlation with the Hα emission for type II Seyfert galaxies. Its origin is very probably the re-emission of very hot dust in a circum-nuclear starburst, since the [25]–[100] colours are similar to those of H II galaxies. Thus diagrams, [25]–[60] versus [25]–[100] and [25]–[100] versus [60]–[100], are also plotted in Figs 4(b) and 4(c), respectively, for sources mentioned above. The power-law line and blackbody line are also plotted. It is seen that same distributions as in Fig. 4(a) can also be found in Figs 4(b) or (c).

Similar discussions in Section 3 for type II quasars are made in the far-infrared. The diagram of far-infrared colour versus redshift and the diagram of the absolute magnitude in 60 μm versus redshift are also plotted in Figs 5 and 6, respectively (the magnitude at 60 μm is defined as $[60] = 0.19–2.5 \log F_{60}$ from the IRAS ES and F_{60} is the flux density in Jy). It is seen from Fig. 5 that no clear relation between the far-infrared colour and the redshift can be found within the $z < 0.3$ domain. However, it is seen from Fig. 6 that the absolute magnitude at 60 μm also increases with redshift. The increase in luminosity with redshift at 60 μm is also a reflection of the flux limit of the *IRAS* survey.

5 SUMMARY

For this paper, almost all type II quasars known so far were collected. Among them 485 sources have *JHK* photometric data, and 65 sources have *IRAS* photometric data in at least one of the three *IRAS*

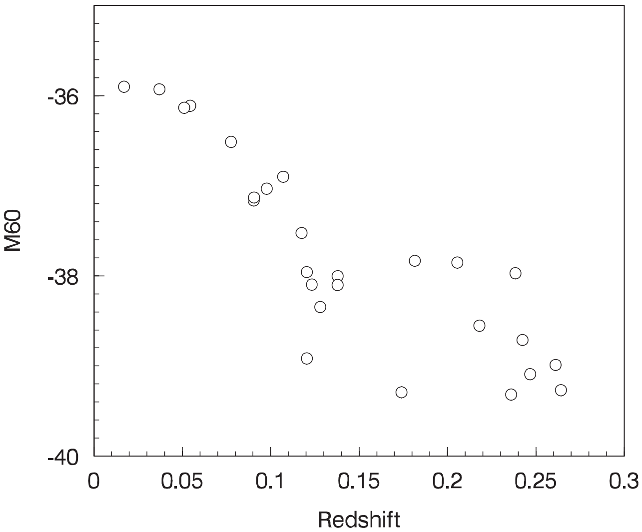

Figure 6. The relation between the absolute magnitude at 60 μm and the redshift for type II quasars.

bands at 25, 60 and 100μm, and 15 sources have *IRAS* photometric data in all three *IRAS* bands.

It is found that nearly half of all type II quasars show thermal starlight radiations from the host galaxies in the near-infrared, as is the case for type II Seyfert galaxies. This result is coincident with the unified scheme for active galactic nuclei. However, over half of all type II quasars show non-thermal core-dominated properties in the near-infrared, as is the case for type I quasars. This result implies that hidden broad lines in the near-infrared may exist for many of those sources. In addition, it is seen that, like type II Seyfert galaxies, both the radiation from the core region and the strong star formation in the host disc may play important roles in the far-infrared. Moreover, the fact that in nearly half of the type II quasars, the infrared emission is dominated by starlight or dust re-emission of starlight, suggests that there might be two classes of type II quasars: in the latter, there would be no BLR, in analogy with the case for type II Seyfert galaxies.

It is also found that no clear relations between infrared colour and redshift can be found either in the near- or far-infrared for type II quasars. However, it is concluded that absolute magnitudes either in the near- or far-infrared all increase with redshift for type II quasars.

ACKNOWLEDGMENTS

We are grateful to the anonymous referee for his/her helpful comments and suggestions. We also thank Dr Zakamska for fruitful discussion about the definition of type II quasars in the optical. This work is supported by grants from the NNSFC (numbers 10503011 and 10533050) and the Chinese Academy of Sciences. This work has made use of the 2MASS data, the NASA ADS database, the NASA/IPAC Extragalactic Database (NED), the CDS SIMBAD database and the CDS VizieR Service.

REFERENCES

Antonucci R., 1993, ARA&A, 31, 473
Barger A. J. et al., 2003, AJ, 126, 632
Beichman C. A., Cutri R., Jarrett T., Stiening R., Skruskie M., 2003, AJ, 125, 2521
Bianchi S., Corral A., Panessa F., Barcons X., Matt G., Bassani L., Carrera F. J., Jimenez-Bailon E., 2008, MNRAS, 385, 195
Boyle B. J., Almaini O., Georgantopoulos I., Blair A. J., Stewart G. C., Griffiths R. E., Shanks T., Gunn K. F., 1998, MNRAS, 297, L53
Brandt W. N., Fabian A. C., Takahashi K., Fujimoto R., Yamashita A., Inoue H., Ogasaka Y., 1997, MNRAS, 290, 617
Caccianiga A. et al., 2004, A&A, 416, 901
Cohen M., Wheaton W. A., Megeath S. T., 2003, AJ, 126, 1090
Crawford C. S., Fabian A. C., Gandhi P., Wilman R. J., Johnstone R. M., 2001, MNRAS, 324, 427
Dadina M., Cappi M., 2004, A&A, 413, 921
de Grijp M. H. K., Lub J., Miley G. K., 1987, A&AS, 70, 95
de Grijp M. H. K., Keel W. C., Miley G. K., Goudfrooij P., Lub J., 1992, A&AS, 96, 387
Della Ceca R. et al., 2003, A&A, 406, 555
Derry P. M., O' Brien P. T., Reeves J. N., Ward M. J., Imanishi M., Ueno S., 2003, MNRAS, 342, 53
Dultzin-Hacyan D., Benitz E., 1994, A&A, 291, 720
Dultzin-Hacyan D., Moles M., Masegosa J., 1988, A&A, 206, 95
Dultzin-Hacyan D., Masegosa J., Moles M., 1990, A&A, 238, 28
Dultzin-Hacyan D., Krongold Y., Fuentes-Guridi I., Marziani P., 1999, ApJ, 513, L111
Dultzin D. et al., 2008, preprint (arXiv:0809.1680)
Fabian A. C. et al., 2000, MNRAS, 315, L8
Gandhi P., Crawford C. S., Fabian A. C., Johnstone R. M., 2004, MNRAS, 348, 529
Gandhi P., Fabian A. C., Crawford C. S., 2006, MNRAS, 369, 1566
Gilli R. et al. (the Cdfs Collaboration), 2002, in Maiolino R., Marconi A., Nagar N., eds, ASP Conf. Ser. Vol. 258, Issues in the Unification of Active Galactic Nuclei. Astron. Soc. Pac., San Francisco, p. 211
Glikman E., Gregg M., Lacy M., Helfand D. J., Becker R. H., White R. L., 2004, ApJ, 607, 60
Gonzalez-Martin O., Masegosa J., Marquez I., Guerrero M. A., Dultzin-Hacyan D., 2006, A&A, 460, 45
Gregg M. D., Lacy M., White R. L., Glikman E., Helfand D., Becker R. H., Brotherton M. S., 2002, ApJ, 564, 133
Gu Q. S., Huang J. H., 2003, in Li X. D., Trimble V., Wang Z. R., eds, Proc. IAU Symp. 214, High Energy Processes and Phenomena in Astrophysics. Astron. Soc. Pac., San Francisco, p. 271
Gu Q. S., Huang J. H., Su H. J., Shang Z. H., 1997, A&A, 319, 92
Gu Q. S., Melnick J., Cid Fernandes R., Kunth D., Terlevich E., 2006, MNRAS, 366, 480
Hyland A. R., Allen D. A., 1982, MNRAS, 199, 943
IRAS Explanatory Supplement., 1988, GPO, Washington, DC (IRAS ES)
Kleinmann S. G., Hamilton D., Keel W. C., Wynn-Williams C. G., Eales S. A., Becklin E. E., Kuntz K. D., 1988, ApJ, 328, 161
Koulouridis E., Plionis M., Chavushyan V., Dultzin-Hacyan D., Krongold Y., Goudis C., 2006a, ApJ, 639, 37
Koulouridis E., Chavushyan V., Plionis M., Krongold Y., Dultzin-Hacyan D., 2006b, ApJ, 651, 93
Koulouridis E., Chavushyan V., Plionis M., Dultzin-Hacyan D., Krongold Y., Goudis C., Chatzichristou E., 2008, Mem. Soc. Astron. Ital., 75, 1
Krongold Y., Dultzin-Hacyan D., 2002, ApJ, 572, 169
Krongold Y., Dultzin-Hacyan D., Marziani P., 2003, Rev. Mex. Astron. Astrofis. Conf. Ser., 17, 105
Lacy M. et al., 2004, ApJS, 154, 166
Lacy M., Canalizo G., Rawlings S., Sajina A., Storrie-Lombardi L., Armus L., Marleau F. R., Muzzin A., 2005, Mem. Soc. Astron. Ital., 76, 154
Leipski C. et al., 2007, A&A, 464, 895
Mainieri V. et al., 2005, MNRAS, 356, 1571
Maiolino R. et al., 2006, A&A, 445, 457
Martinez-Sansigre A., Rawlings S., Lacy M., Fadda D., Jarvis M. J., Marleau F. R., Simpson C., Willott C. J., 2006, MNRAS, 370, 1479
Mouri H., Taniguchi Y., 1992, ApJ, 386, 68
Norman C. et al., 2002, ApJ, 571, 218
Polletta M., Bassani L., Malaguti G., Palumbo G. G. C., Caroli E., 1996, ApJS, 106, 399

Ptak A., Zakamska N. L., Strauss M. A., Krolik J. H., Heckman T. M., Schneider D. P., Brinkmann J., 2006, ApJ, 637, 147
Punsly B., 2006, ApJ, 647, 886
Reyes R. et al., 2008, AJ, 136, 2373
Schlegel D. J., Finkbeiner D. P., Davis M., 1998, ApJ, 500, 525
Schmidt M., Green R. F., 1983, ApJ, 269, 352
Schmidt G. D., Smith P. S., Foltz C. B., Hines D. C., 2002, ApJ, 578, L99
Serjeant S., Rawlings S., Lacy M., McMahon R. G., Lawrence A., Rowan-Robinson M., Mountain M., 1998, MNRAS, 298, 321
Soifer B. T. et al., 1991, ApJ, 381, L55
Stern D. et al., 2002, ApJ, 568, 71
Storchi-Bergmann T., 2008, Rev. Mex. Astron. Astrofis. Ser. Conf., 32, 139
Stoughton C. et al., 2002, AJ, 123, 485
Sturm E., Hasinger G., Lehmann I., Mainieri V., Genzel R., Lehnert M. D., Lutz D., Tacconi L. J., 2006, ApJ, 642, 81
Szokoly G. P. et al., 2004, ApJS, 155, 271
Tran H. D., 2001, ApJ, 554, L19
Urry C. M., Padovani P., 1995, PASP, 107, 803
Veilleux S., Sanders D. B., Kim D.-C., 1997, ApJ, 484, 92
Veilleux S., Sanders D. B., Kim D.-C., 1999, ApJ, 522, 139
Verma A., Charmandaris V., Klaas U., Lutz D., Haas M., 2005, Space Sci. Rev., 119, 355
Vignali C., Alexander D. M., Comastri A., 2004, MNRAS, 354, 720
Vignali C., Alexander D. M., Comastri A., 2006, MNRAS, 373, 321
York D. G. et al., 2000, AJ, 120, 1579
Zakamska N. L., Strauss M. A., Krolik J. H. et al., 2003, AJ, 126, 2125
Zakamska N. L., Strauss M. A., Heckman T. M., Ivezic Z., Krolik J. H., 2004, AJ, 128, 1002
Zakamska N. L. et al., 2005, AJ, 129, 1212
Zakamska N. L. et al., 2006, AJ, 132, 1496

This paper has been typeset from a TEX/LATEX file prepared by the author.